Pharmacological Research 155 (2020) 104725

Contents lists available at ScienceDirect

Pharmacological Research

journal homepage: www.elsevier.com/locate/yphrs

Invited Review

The role of small molecule Flt3 receptor protein-tyrosine kinase inhibitors in the treatment of Flt3-positive acute myelogenous leukemias

Robert Roskoski Jr.

Blue Ridge Institute for Medical Research, 3754 Brevard Road, Suite 116, Box 19, Horse Shoe, NC, 28742-8814, United States

ARTICLE INFO

Chemical compounds studied in this article:
Crenolanib: (PubMED CID: 49803313)
FF10101: (PubMED CID: 90052320)
Gilteritinib: (PubMED CID: 49803313)
Imatinib: (PubMED CID: 5291)
Lestaurtinib: (PubMED CID: 126565)
Midostaurin: (PubMED CID: 9829523)
Ponatinib: (PubMed CID: 24826799)
Quizartinib: (PubMed CID: 24889392)
Sorafenib: (PubMed CID: 216239)
Sunitinib: (PubMed CID: 5329102)

Keywords:
Catalytic spine
Hydrophobic interactions
K/E/D/D
Protein kinase inhibitor classification
Protein kinase structure
Regulatory spine

ABSTRACT

Flt3 is expressed by early myeloid and lymphoid progenitor cells and it regulates the proliferation and differentiation of hematopoietic cells. Flt3 is activated by the Flt3 ligand, the monomeric form of which is a polypeptide of about 200 amino acid residues. Both membrane-associated and soluble Flt3 ligands, which are a product of the same gene, function as noncovalent dimers. *FLT3* mutations occur in about one-third of newly diagnosed acute myelogenous leukemia (AML) patients. This disease is a malignancy of hematopoietic progenitor cells with a variable clinical course; the incidence of this disorder is more than twice that of patients with chronic myelogenous leukemias (20,000 vs. 8500 new patients per year, respectively, in the United States). *FLT3* internal tandem duplication (ITD) results from the head-to-tail duplication of from one to more than 100 amino acids within the juxtamembrane domain and such duplication occurs in about 20–25 % of patients with acute myelogenous leukemias. *FLT3* tyrosine kinase (*FLT3 TK*) mutations, usually within the activation segment, occur in 5–10 % of these patients. The mainstay for the care of acute myelogenous leukemias include daunorubicin or idarubicin and cytarabine. Older patients who are not candidates for such traditional therapy are usually given 5-azacitidine, decitabine, or clofarabine. The addition of orally effective small molecule Flt3 inhibitors to these therapies may prolong event-free and overall survival, a subject of ongoing clinical studies. Midostaurin is US FDA-approved in combination with standard cytarabine and daunorubicin for first-line induction chemotherapy and in combination with cytarabine for second-line consolidation chemotherapy in the treatment of acute myelogenous leukemias with *FLT3*-postive mutations. Moreover, gilteritinib is a Flt3 multikinase inhibitor that is also FDA approved for the care of adult patients with relapsed or refractory acute myelogenous leukemias with *FLT3* mutations. Quizartinib is a Flt3 multikinase inhibitor that was approved by the Ministry of Health, Labor and Welfare (MHLW) of Japan for the treatment of adult patients with relapsed/refractory Flt3-positive acute myelogenous leukemias. Gilteritinib and quizartinib bind to Flt3 with the inactive DFG-D_{out} structure and are classified as type II inhibitors. Furthermore, ponatinib is a multikinase inhibitor that is approved as therapy for Philadelphia chromosome-positive acute lymphoblastic and chronic myelogenous leukemias; it is used off label for the treatment of patients with acute myelogenous leukemias. Moreover, sorafenib is FDA-approved for the treatment of hepatocellular, renal cell, and differentiated thyroid cancers and it is used off label as maintenance therapy following allogeneic hematopoietic stem cell transplantation in the treatment of acute myelogenous leukemias. Other drugs that are in clinical trials for the treatment of this disorder include sunitinib, crenolanib, FF10101, and lestaurtinib. Unlike chronic myelogenous leukemias, which result solely from the formation of the BCR-Abl chimeric protein kinase, acute myelogenous leukemias result from multi-factorial causes and are prone to be resistant to both cytotoxic and targeted therapies. Consequently, there is a pressing need for better understanding the etiologies of acute myelogenous leukemias and for the development of more effective therapies.

Abbreviations: AML, acute myelogenous leukemias; AS, activation segment; CS or C-spine, catalytic spine; CL, catalytic loop; CTT, carboxyterminal tail; D1, immunoglobulin-like domain-1; EGFR, epidermal growth factor receptor; Flt3L, fms-like tyrosine kinase-3 ligand; FGFR, fibroblast growth factor receptor; GIST, gastrointestinal stromal tumors; GK, gatekeeper; GRL, Gly-rich loop; ITD, internal tandem duplication; KD, kinase domain; KID, kinase insert domain; JM, juxtamembrane; NSCLC, non-small cell lung cancers; PDGFR, platelet-derived growth factor receptor; PKA, protein kinase A; PKC, protein kinase C; pY or pTyr, phosphotyrosine; RS or R-spine, regulatory spine; Sh2, shell residue 2; TKD, tyrosine kinase domain; TM, transmembrane; VEGFR, vascular endothelial growth factor receptor

E-mail address: rrj@brimr.org.

https://doi.org/10.1016/j.phrs.2020.104725
Received 23 February 2020; Accepted 24 February 2020
Available online 25 February 2020

1. Functions of the Flt3 receptor and its ligand (Flt3L)

1.1. Flt3 and Flt3L

Protein kinases are catalysts that play a pivotal role in nearly every facet of cell biology and biochemistry [1,2]. These enzymes generate signaling modules that regulate cell cycle progression, proliferation, programmed cell death (apoptosis), cytoskeletal function, motility, differentiation, development, transcription, and translation. Owing to the numerous actions of protein kinases, it is essential that they are carefully regulated because abnormal activity can lead to cancer as well as cardiovascular, inflammatory, and nervous disorders. Because dysregulation, overexpression, and mutations of protein kinases play causal roles in the pathogenesis of human illnesses, these enzymes are attractive drug targets [3].

Protein kinases catalyze the following reaction:

$$MgATP^{1-} + \text{protein–O:H} \rightarrow \text{protein–O:}PO_3^{2-} + MgADP + H^+$$

Based upon the identity of the phosphorylated amino acid, these protein catalysts are cataloged as protein-tyrosine or protein-serine/threonine kinases. Manning et al. documented the existence of 478 typical and 40 atypical protein kinase genes in humans (518 total) as well as 106 pseudogenes [4]. The protein kinase family includes 90 protein-tyrosine kinases, 43 protein-tyrosine kinase-like enzymes, and 385 protein-serine/threonine kinases. Of the 90 protein-tyrosine kinases, thirty-two are non-receptor cytosolic enzymes and 58 correspond to receptors with an extracellular, transmembrane (TM), juxtamembrane (JM), and intracellular domain. A small category of enzymes, including MEK1 and MEK2, are cytosolic dual-specificity protein kinases that catalyze the phosphorylation of threonyl and then tyrosyl residues. These enzymes are evolutionarily related to protein-serine/threonine kinases. The protease family is the largest enzyme family and the protein kinase family is the second largest enzyme family in humans [2]. Manning et al. reported that 244 of 518 protein kinase genes are located at cancer amplicons (gene amplifications) or disease loci [4], a finding that underscores the potential importance of protein kinase antagonists as therapeutic medicinals. The protein-phosphatases mediate phosphoprotein dephosphorylation thereby making protein phosphorylation-dephosphorylation an overall reversible process [5]. This contrasts with regulation by proteases, which is an irreversible one-way process.

Work on Flt3 followed the description of a feline sarcoma virus in 1971 by McDonough et al. [6]. This viral oncogene is called v-FMS (feline McDonough sarcoma) virus. This led to the discovery of the c-FMS proto-oncogene or colony-stimulating factor-1 receptor (CSF1R). Flt1 (fms-like tyrosine kinase-1) is VEGFR1 and Flt2 is fibroblast growth factor receptor-1 (FGFR1). Flt3 (fms-like tyrosine kinase-3) is a membrane-bound receptor protein-tyrosine kinase that plays a crucial role in normal hematopoiesis [7,8]. This protein, which is expressed by early myeloid and lymphoid progenitor cells, regulates the proliferation and differentiation of hematopoietic cells. Flt3 is not expressed in mature hematopoietic cells. *FLT3* mutations occur in about one-third of newly diagnosed acute myelogenous leukemia (AML) patients. *FLT3* internal tandem duplication (ITD) results from the head-to-tail duplication of from one to up to 412 amino acids within the juxtamembrane domain and such duplication occurs in about 20–25 % of patients with AML [9]. The most common sites for duplication occur within the tyrosine-rich region involving codons 589–599. *FLT3* tyrosine kinase (*FLT3 TK*) mutations, usually within the activation segment, occur in 5–10 % of AML patients [10,11]. This gene is also mutated in myelodysplasia and acute lymphoblastic leukemia (ALL) (1–10 %) [8].

Flt3, Kit, macrophage/colony stimulating factor-1 receptor, PDGFRα/β are type III receptor protein-tyrosine kinases. See Refs. [12,13] for a description of the properties of the 20 types of receptor protein-tyrosine kinases. The type III receptors contain an extracellular portion, a transmembrane segment, an intracellular domain that consists of a juxtamembrane segment, a protein kinase domain that contains an insert of several amino acid residues, and a carboxyterminal tail. The extracellular segment contains five immunoglobulin-like domains (D1–D5). The important residues in human Flt3 are listed in Table 1. The extracellular domain, which contains 517 amino acid

Table 1
Important residues in human Flt3[a].

	Flt3	Inferred function	Hanks no.
Signal sequence	1–26		None
Extracellular domain	27–543		None
D1	79–161		None
D2	167–244		None
D3	245–345	Ligand binding	None
D4	348–434		None
D5	435–533		None
TM segment	544–563	Links extracellular and intracellular domains and mediates receptor dimer formation	None
JM segment	564–609	Regulatory and signaling roles	None
JM segment tyrosine phosphorylation sites	572,589,591,599	Regulatory and signaling roles; pY589-Src; pY599-Src	None
Protein kinase domain	610–943	Catalyzes substrate transphosphorylation	I–XI
Glycine-rich loop	^{617}GSGAFG^{622}	Anchors ATP β-phosphate	I
β3-*K* of *K*/E/D/D	K644	Forms salt bridges with ATP α- and β-phosphates and with αC-E	II
αC-*E*, E of K/*E*/D/D	E661	Forms salt bridges with β3-K	III
Hinge-linker residues	^{692}EYCCYGD^{698}	Connects N- and C-lobes and hydrogen bonds with the ATP adenine	V
Kinase insert domain	710–779	Signal transduction	None
Kinase domain tyrosine phosphorylation sites	726, 768,793,842	Interact with a variety of docking proteins that mediate intracellular signaling; pY768-Grb2; pY793-Grb10	
Catalytic loop, HRDLAARN	809–816	Plays both structural and catalytic functions	VIb
Catalytic loop HRD-*D*, First D of K/E/*D*/D	D811	Catalytic base (abstracts protein substrate proton)	VIb
Catalytic loop Asn, HRDLAARN	N816	Chelates Mg^{2+}(2)	VIb
AS DFG-*D*, Second D of K/E/D/*D*	D829	Chelates Mg^{2+}(1)	VII
AS	829–858	Positions protein substrate	VII–VIII
AS tyrosine phosphorylation site	Y842	May stabilizes the AS after phosphorylation or participate in signal transduction	VIII
End of AS	^{856}APE^{858}	Interacts with the αHI loop and stabilizes the AS	VIII
C-terminal tail	944–993	Signal transduction	None
C-terminal tail tyrosine phosphorylation sites	955,969	Mediate intracellular signaling; pY955-Grb2; pY969-Brg2	None
No. of residues	993		
Molecular Wt (kDa)[b]	113		
UniProtKB accession no.	P36888		

[a] AS, activation segment; D1, Immunoglobulin-like domain 1; JM, juxtamembrane; TM, transmembrane.
[b] Unprocessed and non-glycosylated gene product.

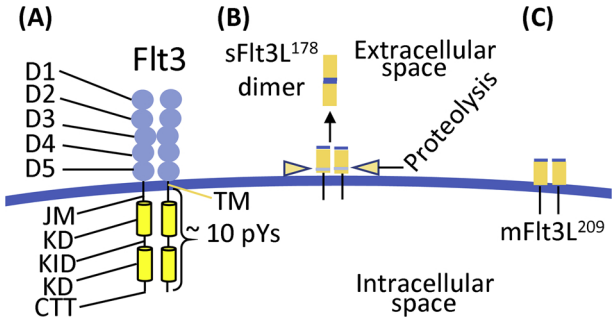

Fig. 1. (A) Overall structure of Flt3. (B) Proteolysis liberates the soluble form of Flt3L, which forms a head-to-head dimer. (C) Membrane-bound Flt3L. D1, immunoglobulin-like domain 1; TM, transmembrane; JM, juxtamembrane; KD, kinase domain; KID, kinase insert domain; CTT, carboxyterminal tail; pY, phosphotyrosine; mFlt3L, membrane-bound Flt3L; sFlt3L, soluble Flt3L.

residues, is longer than the intracellular domain, which contains 430 residues. Additionally, the carboxyterminal tail contains 50 amino acids (944–993). The human Flt3L consists of 235 residues, the amino-terminal 26 residues of which make up the signal peptide. Membrane associated Flt3L contains 209 residues. It can undergo proteolysis as catalyzed by ADAM17 (A disintegrin and metalloproteinase) [8] to generate a soluble form consisting of 178 residues that form active dimers. Membrane-associated and soluble Flt3L are equipotent growth factors. The general architecture of Flt3 and its ligand are depicted in Fig. 1.

The Flt3 ligand (Flt3L), which promotes dimerization and activation of Flt3, consists of a noncovalent dimer that results from hydrophobic and polar interactions [14,15]. The ligand contains four α-helices and two β-strands. The dimeric ligand interacts with the D3 portion of two Flt3 receptors (Fig. 2) with a K_d value of 0.2–0.5 nM. This promotes the phosphorylation of residues in the autoinhibitory JM domain and relieves this inhibition. Additional phosphorylation reactions occur elsewhere that promote the binding of proteins that lead to the activation of the MAP kinase and PKB/AKT signaling modules that result in cell proliferation and inhibition of programmed cell death (apoptosis) [7]. See Ref [8] for a comprehensive discussion of Flt3-mediated signal transduction. In addition to the MAPK and PKB/AKT pathways, Src and Src family kinases, Bruton tyrosine kinase, Syk, and Abl protein kinases

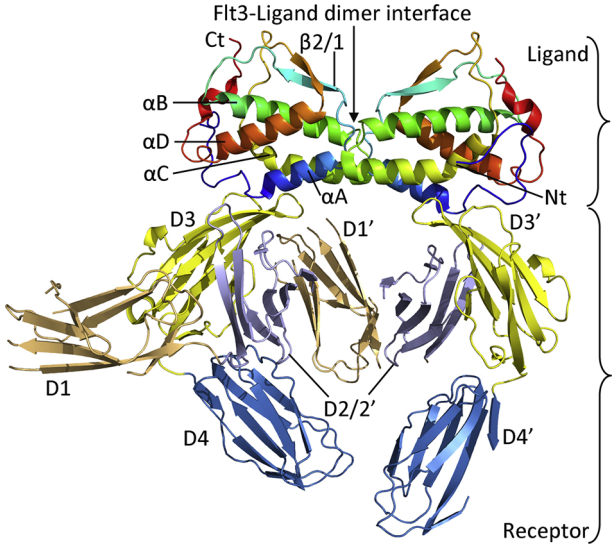

Fig. 2. Flt3 ligand forms a head-to-head dimer as it binds to the Flt3 dimer. Ct, carboxyterminus; D1/1′, immunoglobulin-like domain 1/1′; Nt, amino-terminus. All figures except for 1, 5A, 5B, and 6 were prepared using the PyMOL Molecular Graphics System Version 1.5.0.4 Schrödinger, LLC.

are additional downstream effectors. Flt3 contains 10 tyrosine residues that undergo phosphorylation (Table 1). The order in which these residues become phosphorylated has not been determined [8]. Unlike many protein-tyrosine kinases, phosphorylation of a tyrosine residue within the activation segment is not required for the attainment of maximal enzyme activity.

1.2. Acute myelogenous leukemia

Acute myelogenous leukemia is a malignancy of hematopoietic progenitor cells with a variable clinical course. The expected number of new cases in the United States in 2020 is 19, 940 and the number of deaths is projected to be 11,180 [16]. This represents about 1.1 % of all cancer cases and 1.8 % of all cancer deaths. The incidence of AML is about twice that of chronic myelogenous leukemia (CML) with 8450 new cases and a projected number of deaths in 2020 of 1130 (note the lower death rate for CML as a result of the introduction of imatinib in the treatment of this disorder [2]). Most of the signs and symptoms of people with acute myeloblastic leukemia are due to the replacement of normal bone marrow cells with malignant cells. The patient may have a chief complaint of fatigue; this is often accompanied by easy bruising or bleeding and fever [7]. Laboratory findings include an abnormal bone marrow with at least 20 % blasts, usually accompanied by an elevated peripheral white blood cell count including blasts as well as anemia and thrombocytopenia (decreased platelet count).

Treatment is divided into two phases: remission induction therapy (to attain remission) and post remission or consolidation therapy (to maintain remission) [9]. Remission induction therapy involves a combination of an anthracycline (daunorubicin or idarubicin) and cytarabine. The anthracyclines intercalate with DNA, inhibit the progression of topoisomerase II, and inhibit replication. Cytarabine is converted into cytosine arabinoside triphosphate and is incorporated into DNA where it inhibits both DNA and RNA synthesis. The anthracyclines are administered intravenously over a seven-day period while cytarabine is given by bolus intravenous injection during the first three days (the conventional 7 + 3 regimen). This therapy produces complete remissions in 80–90 % of patients less than 60 years of age and in 50–60 % of older patients. Complete remission refers to the normalization of the bone marrow and peripheral blood count and is not synonymous with a cure. Complete remission is often followed by allogeneic stem cell transplantation.

Older patients who are not candidates for such traditional therapy are usually given 5-azacitidine, decitabine, or clofarabine. 5-Azacitidine and decitabine are analogues of cytidine and deoxycytidine, respectively. They inhibit DNA methyltransferase resulting in the hypomethylation of DNA [17,18]. Abnormal silencing of genes in cancer cells results from hypermethylation of DNA in the promoter regions of tumor suppressors such as Rb, p16, and p73. Decreased methylation of the promoters of tumor suppressor genes restores their expression and inhibits cellular replication. Clofarabine is a purine nucleoside antimetabolite that inhibits ribonucleotide reductase; moreover, following its incorporation into DNA, it promotes DNA polymerase arrest at the replication fork. Addition of Flt3 inhibitors to these therapies may prolong event-free and overall survival, a subject of ongoing clinical studies that are described in Section 5.

2. Properties of the Flt3 receptor protein-tyrosine kinase domain

2.1. Primary, secondary, and tertiary structures of the Flt3 catalytic domain

The catalytic domain of Kit consists of 334 amino acid residues. The average protein kinase domain contains about 275 residues and the larger size of Flt3 is due to the inclusion of a kinase insert domain (KID) of 70 residues [19]. Based upon the amino acid sequences of about five dozen protein-tyrosine and protein-serine/threonine kinases, Hanks and Hunter partitioned protein kinases into 12 domains (I-VIA, VIB-XI)

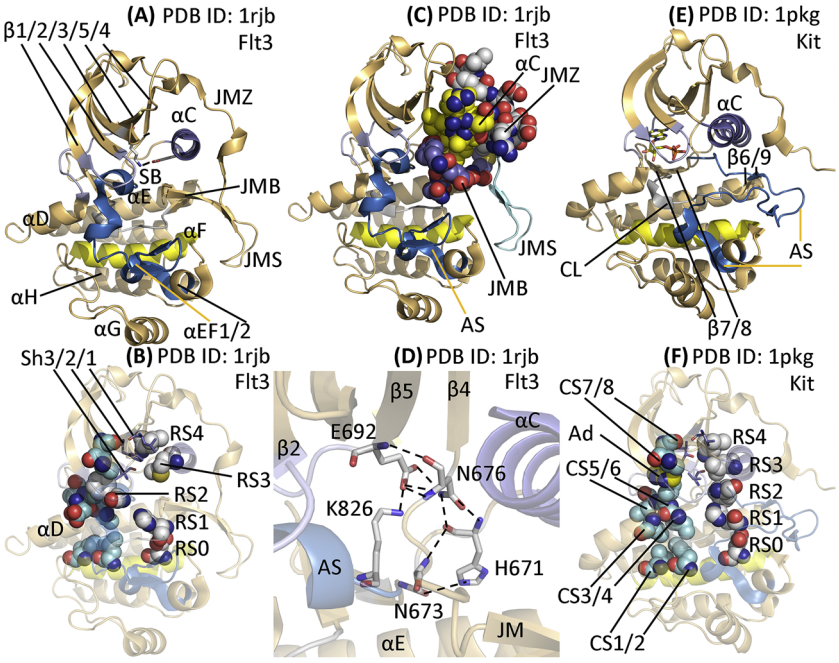

Fig. 3. Overview of the structure of inactive Flt3 (A); the spine residues of inactive Flt3 (B); the JM domain of inactive Flt3 interacting with the αC-helix with the yellow carbon atoms (C); the Flt3 brake interactions (D); overview of active Kit (E); and spine residues of active Kit (F). Dashed lines depict polar bonds. Ad, adenine; AS, activation segment; CL, catalytic loop; CS, catalytic spine; JM, juxtamembrane segment; RS, regulatory spine; SB, salt bridge; Sh, Shell.

[20]. Domain I of Flt3 contains a glycine-rich loop (GRL) with a GxGxΦG signature (^{617}GAGAFG^{622}), where Φ refers to a hydrophobic residue and is phenylalanine in the case of Flt3. The glycine-rich loop connects the β1- and β2-strands that make up part of the roof of the ATP-binding site. The glycine-rich loop, which is a flexible portion of the enzyme, permits both ATP binding and ADP release during the catalytic cycle. Domain II of Flt3 contains a conserved Ala-Xxx-Lys (^{642}AVK^{644}) sequence in the β3-strand and domain III contains a conserved glutamate (E661) in the αC-helix that forms a salt bridge with the conserved β3-lysine in all active protein kinases and many dormant protein kinase conformations (Fig. 3A). Domain V of Flt3 contains a ^{692}EYCCYGD^{698} hinge-linker segment (https://klifs.vu-compmedchem.nl/) that connects the small and large lobes.

Domain VIB within the large lobe of Flt3 contains a conserved HRD sequence, which forms part of the catalytic loop (^{809}HRDLAARN^{816}). The Flt3 domain VII contains an ^{829}DFG^{831} signature and domain VIII contains an ^{856}APE^{858} sequence, which represent the beginning and end of the Flt3 activation segment. This 30-residue segment exhibits different conformations in the active and inactive states. The remaining domains (IX–XI) form the αE–αI helices (Fig. 3A). Most active protein kinases contain αEF1 and αEF2 helices within the activation segment. The X-ray crystallographic structure of the protein kinase A (PKA) catalytic subunit generated an invaluable template for understanding the roles of the 12 Hanks domains and the underlying biochemistry of the entire protein kinase family [21,22]. All protein kinases contain a small N-terminal and a large C-terminal lobe that are connected by the hinge-linker segment [2]. The small lobe contains five conserved β-strands (β1–5) and an important regulatory αC-helix and the large lobe of active enzymes contains seven helices (αD–αI and αEF1/2) along with four conserved β-strands (β6–β9) (Fig. 3). Of the hundreds of protein kinase structures that have been determined, all of them contain the original protein kinase fold as first observed in PKA [2,21,22].

All catalytically active protein kinases contain a K/E/D/D (Lys/Glu/Asp/Asp) amino acid signature that is required for catalysis (Table 1) [2]. The lysine and glutamate occur within the N-terminal lobe and the two aspartate residues occur within the C-terminal lobe. ATP binds in the crevice or cleft between the two lobes and it interacts with each lobe. Comprehensive analyses demonstrate that a salt bridge between the β3-lysine and the αC-glutamate is required for the generation of an active protein kinase conformation, which corresponds to an "αC_{in}" arrangement. These residues in many inactive kinases fail to form this salt bridge and thereby form an inactive "αC_{out}" structure (See Refs. [2] for details). The αC_{in} structure is necessary, but not sufficient, for the expression of protein kinase activity. The activation segment of quiescent Flt3 is in a closed conformation that blocks protein/peptide and ATP binding.

The carboxyterminal lobe contains catalytic loop residues within domain VIb that play important structural and catalytic roles. Moreover, two Mg^{2+} ions function during each catalytic cycle of a number of protein kinases [23,24] and two Mg^{2+} ions are probably required for the proper functioning of Flt3. We infer that Flt3 DFG-D829, the second D of K/E/D/*D*, binds to Mg^{2+}(1); this in turn binds to the β- and γ-phosphate groups of ATP. In the catalytically competent conformation, DFG-D is directed inward toward the active site. Contrariwise, DFG-D of quiescent Flt3 is directed outward producing an inactive DFG-D_{out} structure. Note that the Flt3 X-ray crystallographic structure (PDB ID: 1rjb) was obtained in the absence of any drug so that one cannot argue that a drug induces the DGF-D_{out} conformation.

The 6-amino nitrogen of ADP/ATP forms a hydrogen bond with the carbonyl backbone residue of the first Flt3 hinge-linker residue (E692) that connects the small and large lobes of the protein kinase domain and the *N*1 nitrogen of the adenine base forms a second hydrogen bond with the N−H group of the third hinge residue (C694) (not shown). The adenine binding pocket is located next to these hinge residues. Most orally effective small-molecule steady-state ATP competitive inhibitors of protein kinases, including Flt3, make one or more hydrogen bonds with the backbone residues of the connecting hinge.

The activation segment of protein kinases, which is typically 20–30 residues in length, plays a crucial role that enables catalysis [25]. Its origin is located near the conserved HRD of the catalytic loop and the αC-helix. These structures are interconnected through hydrophobic interactions as part of the regulatory spine as described later. Phosphorylation of one to three residues within the activation segment typically converts a quiescent to a catalytically active protein kinase [26,27]. Flt3 contains a tyrosine within the activation loop (Y842); however, its phosphorylation is not required for enzyme activation. Lemmon and Schlessinger reviewed the mechanisms for receptor protein-tyrosine kinase activation and this process generally requires growth factor-induced formation of receptor dimers and subsequent protein kinase activation following enzyme phosphorylation [13]. Under physiological conditions, Flt3L binds to D3 of two monomers to promote receptor dimerization [15]. Following dimerization, one

member of the dimer pair mediates the phosphorylation of inhibitory JM domain tyrosine residues of the receptor partner (in *trans*); this is followed by the phosphorylation of other protein-tyrosines in turn creating docking sites for signal transduction proteins [8]. Phosphorylation of the JM domain relieves inhibition and initiates additional protein-tyrosine phosphorylation. Note that the *FLT3 ITD* mutations occur within the JM domain and the resulting enzyme activation is presumably related to the disruption of physiological JM domain inhibition.

Chen et al. described the inhibition of FGFR2 by an intramolecular autoinhibitory brake [28]. Flt3, Kit, VEGFR1/2/3, FGFR1/3/4, PDGFRα/β, Kit, CSF1R, Tek, and Tie protein kinases are also regulated by a similar autoinhibitory mechanism. This process involves a KEN triad consisting of three main residues: a lysine (K) in the β8-strand, a glutamate (E) corresponding to the second hinge residue, and an asparagine (N) within the αC-β4 back loop. The intricate hydrogen bonding pattern for these three residues in Flt3 is illustrated in Fig. 3D. A hydrogen bond forms between the side chain of K826 and the carboxylate side chain of E692 and another occurs between the carboxylate side chain of E692 and the backbone N−H group of N676. The N−H group of E692 hydrogen bonds with the carbonyl group of N676. Moreover, two polar bonds link the carboxylate side chain of E692 with the amide side chain of N676. The carboxylate side chain of E692 also hydrogen bonds with the backbone N−H group of N676. Additionally, the ε-amino group of K826 and the amide side chain of N676 also form polar bonds with the carbonyl oxygen of I544 within the αC-β4 back loop (not shown). The side-chain carbonyl group of N673 also hydrogen bonds with H671 within the back loop (Fig. 3D). Only three of the ten polar bonds observed in the autoinhibitory brake are conserved in the active enzyme with a disengaged brake (not shown).

The Flt3 HRDLAARN catalytic-loop aspartate (D811), which is the first D of the K/E/*D*/D signature, functions as a Lowry-Bronsted base and removes a proton from the protein-tyrosine-substrate −OH group; this enables the nucleophilic attack of the oxygen atom onto the γ-phosphorus atom of ATP (Fig. 4) [29]. An open activation segment positions the protein substrate and promotes catalysis. β3-K644 forms salt bridges with αC-E661 and the α- and β-phosphates of ATP. Based upon studies with PKA [2,24], Mg^{2+}(1) binds to the β- and γ-phosphates while Mg^{2+}(2) binds to the α- and γ-phosphates of ATP thereby promoting catalysis. The catalytic segment AAR sequence occurs in many receptor protein-tyrosine kinases including Flt3, Kit, colony-stimulating factor-1 receptor, EGFR, and PDGFRα/β while RAA occurs in

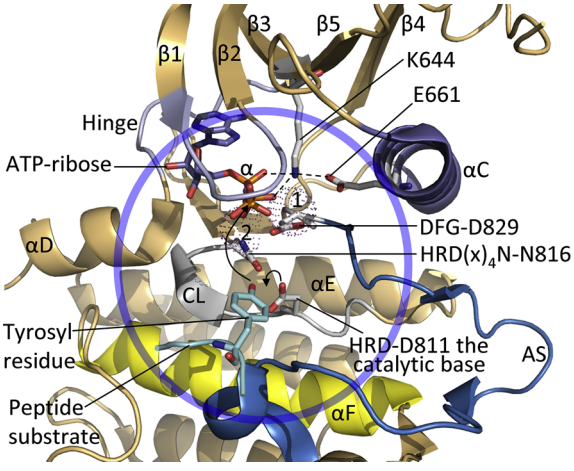

Fig. 4. Inferred mechanism of the Flt3-catalyzed protein kinase reaction. HRD-D811 abstracts a proton from the protein tyrosyl substrate allowing for its nucleophilic attack onto the γ-phosphorus of ATP. The chemistry occurs within the circle. 1 and 2 label the two Mg^{2+} ions shown as dots. AS, activation segment; CL, catalytic loop; The figure was prepared from FGFR2 (PDB ID: 2PVF), but the residue numbers correspond to those of human Flt3.

many nonreceptor protein-tyrosine kinases such as Src [20]. However, the functional significance of this difference in the catalytic loop structure is unclear.

2.2. The hydrophobic spines of Flt3

Kornev et al. examined the structures of 23 protein kinases and they determined the role of several critical residues by a local spatial pattern alignment algorithm [30,31]. They described (i) eight hydrophobic residues as a catalytic or C-spine and (ii) four hydrophobic residues as a regulatory or R-spine. Both spines contain amino acid residues from both the N-terminal and C-terminal lobes. The R-spine contains one residue from the activation segment (DFG-F) and another from the regulatory αC-helix, both of which are major regulatory components that assume active and quiescent conformations. The base of the R-spine within the carboxyterminal lobe anchors the activation segment and catalytic loop in an active state and the C-spine positions ATP in the active site thereby promoting catalysis. Moreover, the proper alignment of each spine is required for the assembly of an active enzyme.

The importance of the interaction of therapeutic protein kinase antagonists with the R-spine, the C-spine, and the shell residues is widespread and cannot be overstated. For a listing of the properties of the spine and shell residues as well as their interactions with various inhibitors of the ALK receptor protein-tyrosine kinase, see Refs. [32,33]; for B-Raf protein-serine/threonine protein kinase, see Refs. [34,35]; for Bruton non-receptor protein-tyrosine kinase, see Ref. [36]; for the cyclin-dependent protein-serine/threonine kinases, see Refs. [37,38]; for the ERK1/2 protein-serine/threonine protein kinases, see Refs. [39,40]; for the EGFR/ErbB receptor protein-tyrosine kinases, see Refs. [41,42]; for the Janus non-receptor protein-tyrosine kinases, see Ref. [43]; for the dual specificity MEK1/2 enzymes, see Refs. [44,45]; for the PDGFRα/β protein-tyrosine kinases, see Ref. [46]; for the RET receptor protein-tyrosine kinase, see Ref. [47]; for the ROS1 orphan-receptor protein-tyrosine kinases, see Ref. [48]; for the Src non-receptor protein tyrosine kinase, see Ref. [23]; for the VEGFR1/2/3 protein-tyrosine kinases see Ref. [49]; and for the FGFR protein-tyrosine kinases, see Ref. [50].

Going from the base to the apex, the protein kinase R-spine consists of the catalytic loop HRD-H, the activation segment DFG-F, the amino acid four residues C-terminal to the conserved αC-glutamate, and the amino acid at the beginning of the β4-strand [30]. The backbone N−H group of the HRD-H forms a salt bridge with a conserved aspartate carboxylate group within the αF-helix. Again, going from the base to the apex of the R-spine, Meharena et al. designated the R-spine residues as RS0, RS1, RS2, RS3, and RS4 (Fig. 3B/F) [51]. The R-spine of dormant enzymes such as Flt3 with DFG-D_{out} is nonlinear and broken with a displaced RS2 residue (Fig. 3B). In contrast, the R-spine of active Kit with DFG-D_{in} is linear (Fig. 3F) (See Refs. [2,52] for details). The C-spine of protein kinases contains amino acid residues from both the N-terminal and C-terminal lobes and the adenine base of ATP completes this spine (Fig. 3F) [31]. The two residues within the small lobe that interact with the ATP adenine include a conserved valine at the beginning of the β2-strand (CS7) and an invariant alanine from the AxK signature of the β3-strand (CS8). Moreover, a residue from the β7-strand (CS6) on the floor of the adenine pocket interacts hydrophobically with the ATP adenine. Based upon the examination of dozens of crystal structures, basically all steady-state ATP-competitive protein kinase antagonists interact with CS6. The CS6 residue occurs between two hydrophobic residues (CS4 and CS5) that form part of the β7-strand and CS6 interacts with the CS3 residue near the initial portion of the αD-helix of the large lobe. CS5/6/4 occur immediately after the catalytic loop asparagine (HRDxxxxN) so that these residues can be easily identified within the primary structure. The CS3 and CS4 residues interact with CS1 and CS2 of the αF-helix to complete the C-spine (Fig. 3B/F) [31]. Note that the αF-helix, which spans the base of the entire large lobe, anchors both the C- and R-spines. Moreover, both

spines play a central role in securing the protein kinase catalytic residues in an active state. CS7 and CS8 in the small lobe make up part of the "ceiling" of the adenine-binding pocket while CS6 in the large lobe makes up part of the "floor" of the binding pocket.

Based upon the findings of site-directed mutagenesis studies, Meharena et al. described three shell (Sh) residues in the PKA catalytic subunit that reinforce the R-spine, which they labeled Sh1, Sh2, and Sh3 [51]. The Sh2 residue represents the proverbial gatekeeper residue of protein kinases. The gatekeeper residue plays a critical role in controlling access to the back pocket [53,54] or hydrophobic pocket II (HPII) [54,55]. In contrast to the identification of the DFG, APE, or HRD signatures, which is based upon the amino acid sequence [20], the two spines were identified by their three-dimensional location in active or dormant protein kinases [30,31]. Table 2 provides a compilation of the spine and shell residues of Flt3. Small molecule protein kinase inhibitors regularly interact with residues within the R-spine, C-spine, and shell residues [52].

3. Inhibitor classification

Dar and Shokat divided protein kinase antagonists into three groups, which they labeled as types I, II, and III [56]. They classified type I inhibitors as those that bind within and around the adenine pocket of a catalytically active enzyme. Moreover, they classified type II inhibitors as those that bind to an inactive DFG-D_{out} protein kinase and they classified type III inhibitors as agents that bind to an allosteric site that does not overlap with the adenine-binding pocket. Subsequently, Zuccotto defined type I½ inhibitors as those compounds that bind to an inactive protein kinase with a DFG-D_{in} structure [57]. Such an inactive enzyme may display a closed activation segment, a non-linear or broken R-spine, an abnormal glycine-rich loop, an autoinhibitory brake, an αC_{out} conformation, or various combinations of these structural parameters. Furthermore, Gavrin and Saiah subdivided allosteric inhibitors into types III and IV [58]. The type III inhibitors bind within the crevice between the small and large lobes and next to, but not overlapping, the ATP binding site. In contrast, type IV inhibitors bind outside of the crevice between the small and large lobes. Additionally, Lamba and Gosh defined compounds that span two distinct regions of the protein kinase domain as bivalent or type V inhibitors [59]. For example, a compound that binds to (i) the SH2 domain and (ii) adenine-binding pocket of Src would be classified as a type V inhibitor [60]. To complete the inhibitor classification, we classified type VI inhibitors as those ligands that form a covalent bond with their target enzyme [52]. For example, afatinib binds covalently to mutant *EGFR* and is approved for the treatment of NSCLC. Mechanistically, this medicinal initially binds like a type I inhibitor to active EGFR and then the C797 –SH group of the enzyme attacks the drug to form a type VI covalent adduct (PDB ID: 4g5j) [52].

We previously classified type I½ and type II inhibitors into A and B subtypes [52]. Type A inhibitors are drugs that extend past the Sh2 gatekeeper residue into the back cleft. In contradistinction, type B antagonists are medicinals that do not extend into the back cleft. Based upon preliminary results, the potential importance of this distinction is that type A inhibitors bind to their target enzyme with longer residence times [61] when compared with type B inhibitors [52]. Sunitinib is a type IIB VEGFR inhibitor that is approved by the FDA for the treatment of renal cell carcinomas. Sorafenib is a type IIA VEGFR antagonist that is also approved by the FDA for the treatment of these carcinomas. The type IIB inhibitor has a residence time of less than 2.9 min while that of the type IIA inhibitor has a residence time that is 20-fold greater (64 min) [52].

Table 2
Spine and shell residues of human Flt3 and Kit.

	Symbol	KLIFS No.[a]	Flt3	Kit
Regulatory spine				
β4-strand (N-lobe)	RS4	38	L677	L656
C-helix (N-lobe)	RS3	28	M665	L644
Activation loop F of DFG (C-lobe)	RS2	82	F830	F811
Catalytic loop His (C-lobe)	RS1	68	H809	H790
F-helix (C-lobe)	RS0	None	D870	D851
R-shell				
Two residues upstream from the gatekeeper	Sh3	43	L689	V668
Gatekeeper, end of β5-strand	Sh2	45	F691	T670
αC-β4 loop	Sh1	36	V675	V654
Catalytic spine				
β3-AxK motif (N-lobe)	CS8	15	A642	A621
β2-strand (N-lobe)	CS7	11	V624	V603
β7-strand (C-lobe)	CS6	77	L818	L799
β7-strand (C-lobe)	CS5	78	V819	L800
β7-strand (C-lobe)	CS4	76	V817	I798
D-helix (C-lobe)	CS3	53	L699	L678
F-helix (C-lobe)	CS2	None	L877	F858
F-helix (C-lobe)	CS1	None	I881	L862

[a] KLIFS (kinase–ligand interaction fingerprint and structure) from Ref. [62].

4. Drug binding pockets

Liao [55] and van Linden et al. [62] divided the region between the small and large lobes of protein kinases into the front cleft (front pocket), the gate area, and the back cleft. A general overview illustrating these sites and various sub-pockets is provided in Fig. 5 and Table 3. The gate area and back cleft make up the back pocket or HPII (hydrophobic pocket II). The front cleft contains the final three residues of the β1-strand, the entire glycine-rich loop, the initial four residues of the β2-strand, the hinge-linker segment and the αD-strand, the catalytic loop, and the β7-strand within the large lobe. Type I inhibitors typically bind within the front cleft. The gate area is made up of the three residues at the end of the β3-strand, the first two residues of the β3-αC loop, the residue immediately before the activation segment (the x residue of xDFG), and the initial four residues of the activation segment. The back cleft contains the middle of the αC-helix, the β4-strand, the final two residues of the β5-strand, the first two and the fifth residue from the αE-helix, and the two residues immediately before the catalytic loop (Fig. 5C). Many type I½ inhibitors occupy both the front cleft and the initial part of the back cleft. One of the prospective goals in the formulation of small molecule protein kinase inhibitors is to establish selectivity in order to reduce off-target side effects [63]; this process is facilitated by evaluating the interaction of drugs with their target enzymes [64–66]. Fabricating drug scaffold appendages that bind to residues lining the sub-pockets within the cleft plays a tactical role in protein kinase inhibitor drug discovery and development with the goal of achieving maximal drug affinity.

van Linden et al. formulated a comprehensive catalog of ligand and drug binding to more than twelve hundred human and mouse protein kinases [62]. The KLIFS (kinase–ligand interaction fingerprint and structure) listing includes a grouping of 85 possible ligand binding-site residues that occur in both lobes [63]. The listing helps in the discovery of related interactions and aids in the classification of drugs and ligands based upon their binding properties. Moreover, these authors formulated a universal amino acid residue numbering system that facilitates a comparison of different drug-kinase interactions [62]. Table 2 lists the correspondence between the KLIFS database residue nomenclature and the C-spine, R-spine, and shell residue numbers. Moreover, these investigators established a useful non-commercial and searchable web site, which they regularly update, that describes the interaction of human and mouse protein kinases with ligands and drugs (klifs.vu-compmedchem.nl/).

5. Drug-enzyme interactions

Gilteritinib is a pyrazinecarboxamide derivative (Fig. 6A) and a Flt3

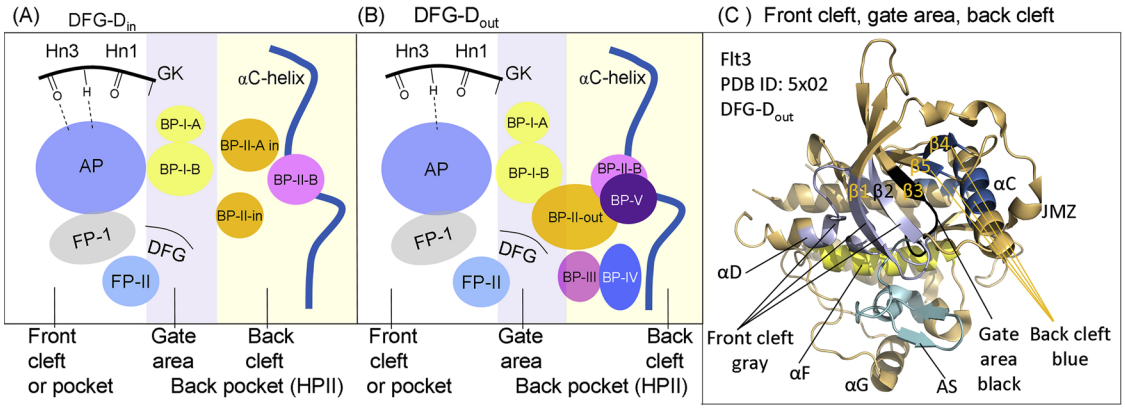

Fig. 5. Location of the protein kinase domain drug-binding pockets. AP, adenine pocket; BP, back pocket; FP, front pocket; Hn, hinge; HPII, hydrophobic pocket II. Adapted from Refs. [55,62].

Table 3
Location of selected protein kinases cleft and gate area residues.

Description	Location	KLIFS residue no.[a]
GxGxΦG	Front cleft	4–9
β2-strand V (CS7)	Front cleft	11
β3-strand A (CS8)	Front cleft	15
HRD with DFG-D$_{in}$	Front cleft	68–70
HRD(x)$_4$N-N	Front cleft	75
β7-strand CS6	Front cleft	77
β3-strand K	Gate area	17
αC-β4 penultimate back loop residue	Gate area	36
Gatekeeper residue	Gate area	45
The x of xDFG	Gate area	80
DFG	Gate area	81–83
αC-helix E	Back cleft	24
RS3	Back cleft	28
HRD with DFG-D$_{out}$	Back cleft	68–70

[a] Ref. [62].

multikinase inhibitor that is US FDA approved for the treatment of adult patients with relapsed or refractory AML with a *FLT3* mutation as detected by the FDA-approved LeukoStrat CDx mutation assay [67]. Besides Flt3, the drug inhibits the ALK, LTK, ROS1, and RET receptor protein-tyrosine kinases with IC_{50} values in the low nanomolar range [68]. The X-ray crystal structure of gilteritinib bound to Flt3 demonstrates that a carboxamide N−H group forms a hydrogen bond with the carbonyl group of E692 (Fig. 7A) and the carboxamide carbonyl moiety form a hydrogen bond with the N−H group of C694 (the third hinge residue). The drug makes hydrophobic contact with four spine residues (RS2, CS6/7/8) but none of the shell residues (Table 4). The pharmaceutical interacts hydrophobically with the β1-strand residue immediately preceding the glycine-rich loop (L616); this residue corresponds to KLIFS-3 (kinase–ligand interaction fingerprint and structure residue-3). The drug makes hydrophobic contact with Y693, C694, and C695 of the hinge as well as C828 (the x of xDGF) and DFG-D829. The 4-methylpiperazine helps to solubilize the drug and it extends from the enzyme into the solvent front. The therapeutic occupies the front cleft only. The compound is bound to a DFG-D$_{out}$ inactive conformation of Flt3 with the autoinhibitory brake and the activation segment in a closed conformation. Overall this interaction corresponds to that of a type IIB inhibitor [52]. See Ref [67] for a summary of the clinical trials that led to its approval in Japan and the United States in 2019.

Quizartinib is a benzothiazole-phenyl urea derivative (Fig. 6B) that was approved by the Ministry of Health, Labor and Welfare (MHLW) of Japan for the care of adult patients with relapsed/refractory *FLT3-ITD* acute myelogenous leukemias as detected by an MHLW-approved test. This medicinal is a second-generation Flt3 inhibitor that possesses activity against Kit, PDGFR, and RET [69]. Its more potent inhibitory power against Flt3 when compared with first generation inhibitors was evident in studies of patients with acute myelogenous leukemias treated with single agent quizartinib, in which complete response rates were greater than 40 %. Midostaurin, crenolanib, and quizartinib lack significant activity against *Flt3-TKD* mutant proteins in contrast to gilteritinib. The generation of TKD mutants is an established mechanism of resistance in quizartinib-treated patients as well as a primary cause of 5–10 % of cases of acute myelogenous leukemias.

The X-ray crystal structure of quizartinib bound to Flt3 shows that the sulfur atom of benzothiazole forms a weak hydrogen bond with the N−H group of C694 (the third hinge residue). This contrasts with most small molecule protein kinase inhibitors where strong hydrogen bonds involving drug (i) nitrogen or (ii) oxygen form with hinge amino acid residue carbonyl or N−H groups. The N−H groups of the quizartinib ureido moiety form hydrogen bonds with αC-E661 and the oxygen atom of the ureido moiety forms a hydrogen bond with the N−H group of DFG-D829 (Fig. 7B). The therapeutic makes hydrophobic contact with six spine residues (RS1/2/3, CS6/7/8), two shell residues (Sh1/2), and KLIFS-3 (Table 4). The medicinal makes hydrophobic contact with β3 AVK-K644, αC-residues E661, M664, and M665; it makes additional hydrophobic contact with I674 and V675 of the αC-β4 back loop. Moreover, the drug makes hydrophobic contact with Y693, C694, C695, Y696 within the hinge-linker segment, I827 within the β8-strand, C828 (the x of xDFG), DFG-D829, and A833 within the activation segment. The drug occurs in the front pocket, gate area, back pocket, BP-I-B, BP-II-out, BP-III (Table 4). The morpholino group helps to solubilize the drug and it extends from the enzyme into the solvent. The compound is bound to a DFG-D$_{out}$ inactive conformation of Flt3 with the autoinhibitory brake and the activation segment in a closed conformation and it extends well into the back cleft. Overall this interaction corresponds to that of a type IIA inhibitor [52]. See Ref [69]. for a summary of the clinical trials that led to its approval in Japan.

FF10101 is an anilino-pyridine derivative (Fig. 6C) with potent inhibitory power against Flt3 and FMS with IC_{50} values in the sub-nanomolar range; it inhibits Kit and FGFR with IC_{50} values an order of magnitude greater [70]. The medicinal antagonizes Flt3 bearing internal tandem duplications within the JM domain as well as activation segment mutations, both classes of mutations that lead to constitutive Flt3 activation. The drug inhibits the growth of primary AML cells in culture and in xenografts and is in two clinical trials in patients with AML (ClinicalTrials.gov). The X-ray crystal structure of the drug show that the pyrimidine *N*1 forms a hydrogen bond with the N−H group of the third hinge residue (C694), the 2-amino-pyrimidine group forms a hydrogen bond with E692, and the 4-cyano group forms a hydrogen bond with AVK-K644 (Fig. 7C). F10101 also forms a covalent bond with C694. The drug makes hydrophobic contact with four spine residues (RS2, CS6/7/8), two shell residues (Sh1/2), and the KLIFS-3 residue. It

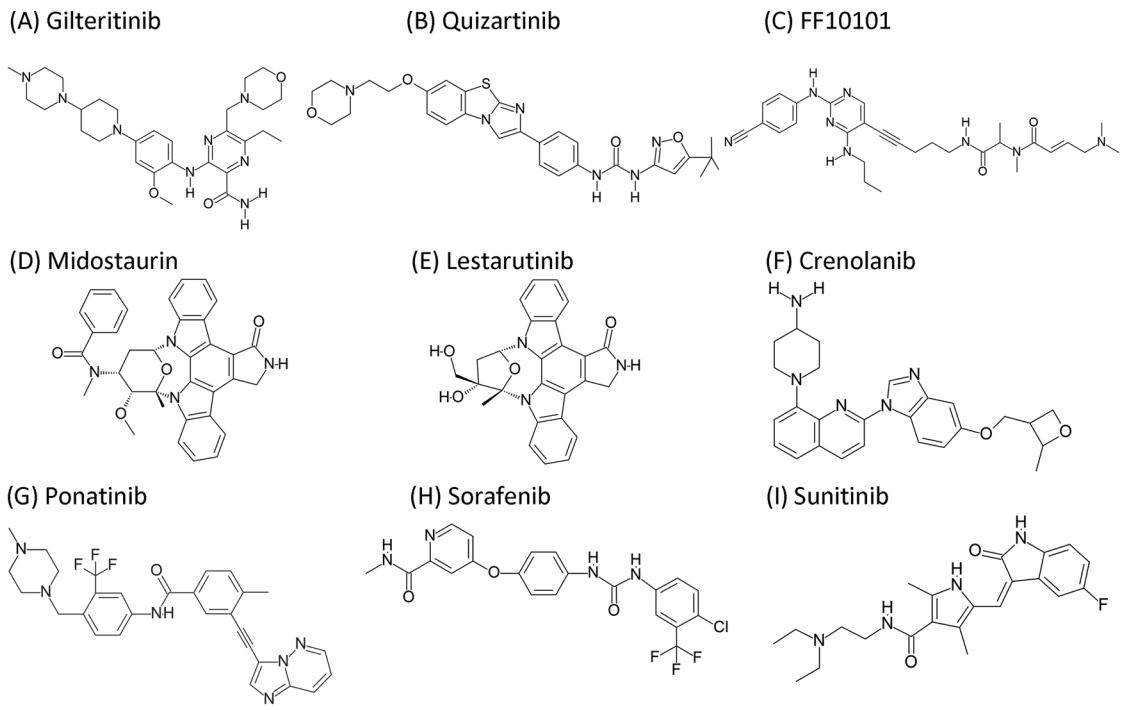

Fig. 6. Structures of selected Flt3 receptor multikinase inhibitors.

also makes hydrophobic contact with AVK-K644, V675 of the back loop, Y693, C694, C695, Y696, and D698 of the hinge-linker segment, and C828 (the x of xDFG). The drug occupies the front cleft, gate area, back cleft, and BP-I-B. The compound is bound to a DFG-D_{out} inactive conformation of Flt3 with the autoinhibitory brake and the activation segment in a closed conformation. This resembles a type IIB inhibitor; however, because the drug is bound covalently, it is classified as a type VI inhibitor. The drug is in its early clinical stages of development; time will tell whether it will become approved by health authorities for clinical use.

Midostaurin is a derivative of staurosporine [71], which is a bacterially (*Streptomyces stauroporeus*) expressed alkaloid that inhibits many protein kinases (a pan-protein kinase inhibitor) including Flt3 [72]. This indolocarbazole derivative (Fig. 6D) is FDA-approved in combination with standard cytarabine and daunorubicin for induction and cytarabine for consolidation in the treatment of acute myelogenous leukemias with *FLT3*-postive mutations as detected by the FDA-approved test. Induction therapy represents the first-line therapy and consolidation therapy is given once a remission has been achieved with the goal of sustaining the remission. Midostaurin is also approved as a first-line treatment of (i) aggressive systemic mastocytosis, (ii) systemic mastocytosis with associated hematologic neoplasms, and (iii) mast cell leukemias [73–75]. This drug was initially developed as a PKC serine/threonine kinase inhibitor, but it is a potent antagonist of several receptor and non-receptor protein kinases including BCR-Abl, BCR-Abl T315I, VEGFR, FGFR, EphR, Src family kinases, Kit, PDGFRα/β, RET, and Tie2 [76].

We lack the X-ray crystal structure of midostaurin bond to Flt3; however, we have the structure of the drug bound to DYRK1A [77], a dual specificity protein kinase, that we can use as a template for its possible interactions with Flt3. The *N*1 pyrrolo N—H group forms a hydrogen bond with the carbonyl group of E239 and the pyrrolo carbonyl group forms a hydrogen bond with the N—H group of L241 (the third hinge residue) (Fig. 8A). The medicinal makes hydrophobic contact with three spine residues (CS6/7/8), two shell residues (Sh1/2), and KLIFS-3. The drug makes hydrophobic contact with F170 within the G-rich loop, AIK-K188, M240 (the second hinge residue), Y246 within the αD-helix, E291 of the catalytic loop, V306 (the x of xDFG), and DFG-D307. Midostaurin binds in the front pocket including FP-II and it does not extend into the gate area. Midostaurin binds to an active enzyme with a phosphorylated and open activation segment and it is classified as a type I inhibitor [52]. Biochemical studies indicate that midostaurin binds to an active Flt3 and it is possible that the interaction of the compound with Flt3 may have much in common with its

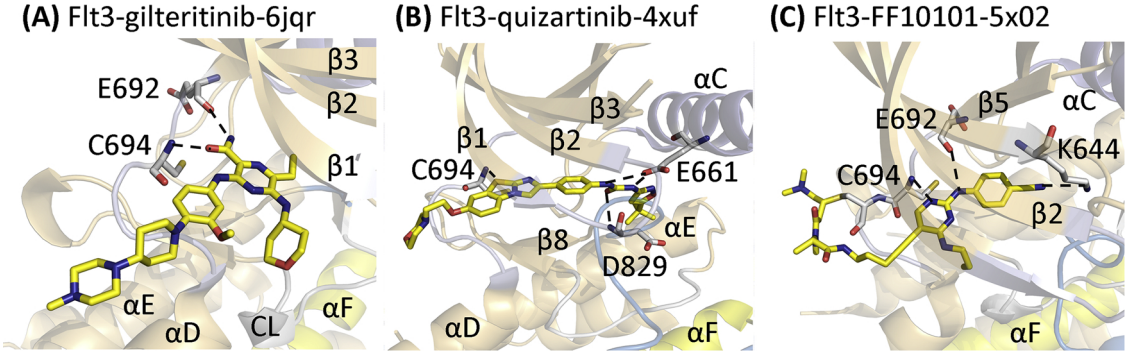

Fig. 7. Structures of Flt3-drug complexes. The carbon atoms of the drugs are colored yellow. AS, activation segment; CL, catalytic loop; GK, gatekeeper. The dashed lines depict hydrogen bonds.

Table 4
Human drug-enzyme hydrophobic (Φ) interactions using their designated KLIFS residue numbers[a].

	PDB ID	Inhibitor type	RS1	RS2	RS3	Sh1	Sh2	Sh3	CS6	CS7	CS8	KLIFS-3	KLIFS pockets[b] & subpockets
KLIFS no. →			68	82	28	36	45	43	77	11	15	3	
Drug-enzyme ↓													
Flt3-gilteritinib	6jqr	IIB		Φ					Φ	Φ	Φ	Φ	F
Flt3-quizartinib	4xuf	IIA	Φ	Φ	Φ	Φ	Φ		Φ	Φ	Φ	Φ	F, G, B, BP-I-B, BP-II-out, BP-III
Flt3-FF10101	5x02	VI (IIB)		Φ		Φ	Φ		Φ	Φ	Φ	Φ	F, G, B, BP-I-B
PKC-midostaurin	4nct	I				Φ	Φ		Φ	Φ	Φ	Φ	F, FP-II
PRK1-lestaurtinib	4otg	I				Φ	Φ		Φ	Φ	Φ	Φ	F
CAMKK2B-crenolanib	6bqp	IIA				Φ	Φ		Φ	Φ	Φ	Φ	F, FP-I
Kit-ponatinib	4u0i	IIA	Φ	Φ	Φ	Φ	Φ	Φ	Φ	Φ	Φ	Φ	F, G, B, BP-I-A/B, BP-II-out, BP-III/IV
VEGFR2-sorafenib	4asd	IIA	Φ	Φ	Φ	Φ	Φ		Φ	Φ	Φ	Φ	F, G, B, BP-I-B, BP-II-out, BP-III
VEGFR2-sunitinib	4 agd	IIB		Φ		Φ	Φ		Φ	Φ	Φ	Φ	F, BP-I-B

[a] KLIFS-3, kinase-ligand interaction fingerprint and structure residue-3; from http://klifs.vu-compmedchem.nl/.
[b] F, front pocket; G, gate area; B, back pocket [62].

interaction with DYRK1A.

Lestaurtinib is another indolocarbazole derivative (Fig. 6E) and a first-generation Flt3 multikinase inhibitor that is or has been in five clinical trials in patients with AML (ClinicalTrials.gov). Other disease targets include myelofibrosis, polycythemia vera, neuroblastoma, and prostate cancer. It was initially developed as a TRKA inhibitor [78]. Its other known enzyme targets include PKC, PDGFR, and VEGFR2 [68,79]. We lack the X-ray crystal structure of the drug bound to Flt3; however, we have the structure of lestaurtinib bound to PRK1 (PKN1), a PKC-like serine/threonine kinase [80]. The structure shows that the N−H group of the drug forms a hydrogen bond with the carbonyl group of E702 and the carbonyl group of the drug forms a hydrogen bond with the N−H group of S704 (the third hinge residue). The medicinal makes hydrophobic contact with three spine residues (CS6/7/8), two shell residues (Sh1/2), and the KLIFS-3 residue (Table 4). It also makes hydrophobic contact with R629 and F632 of the G-rich loop, AIK-K650 of the β3-strand, Y703, S704, A705, D708 of the hinge-linker segment connecting the small to the large lobes, A763 (the x of xDFG), and DFG-D764 (Fig. 8B). Lestaurtinib binds to the front pocket of an active enzyme with a phosphorylated threonine within its open activation segment and is therefore classified as a type I inhibitor [52]. Biochemical studies indicate that the compound binds to an active Flt3 and it is conceivable that the interaction of the compound with Flt3 may have much in common with its interaction with PKN1. Whether lestaurtinib will be approved for the treatment of AML is unlikely owing to the lack of any overall benefit in a phase III trial when combined with chemotherapy in patients with newly diagnosed AML bearing *FLT3-ITD* mutations [81,82].

Crenolanib is a quinoline derivative (Fig. 6F) and a second-generation Flt3 multikinase inhibitor that is in 12 clinical trials for the treatment of AML (ClinicalTrials.gov); it is also in clinical trials targeting GIST, gliomas, and glioblastomas. This agent also targets Kit, PDGFR, and RET [68]. We lack the X-ray crystal structure of the drug bound to Flt3; however, we have the structure of the drug bound to CAMKK2B, a calcium-calmodulin dependent protein serine/threonine kinase [83]. The structure shows that *N*1 of the quinoline moiety forms a hydrogen bond with the N−H group of V270 (the third hinge residue) and the 4-amino group hydrogen bonds with the S316 hydroxyl group within the catalytic loop (Fig. 8C). The compound makes hydrophobic contact with three spine residues (CS6/7/8), two shell residues (Sh1/2), and the KLIFS-3 residue in the β1-strand. The drug also makes hydrophobic contact with K173 within the glycine-rich loop, AMK-K194 of the β3-strand, E268, L269, V270, Q272, P274 of the hinge-linker segment, S316 of the catalytic loop, A329 (the x of xDFG), and DFG-D330. The drug occupies the front pocket and FP−I. It binds to an active enzyme with an open activation segment and is classified as a type I inhibitor. Biochemical studies indicate that crenolanib binds to active Flt3 and the structure of the drug-CAMKK2B complex may reflect its mode of interaction with Flt3. Unlike the case for lestaurtinib, the clinical trials of crenolanib are more promising [82].

Ponatinib is an imidazo-pyridazine (Fig. 6G) multikinase inhibitor that is approved for the treatment of Philadelphia chromosome-positive acute lymphoblastic and chronic myelogenous leukemias (Supplementary material); it is undergoing clinical trials for the treatment of various hematologic neoplasms including nine that are directed against AML as well as GIST and other solid tumors (ClinicalTrials.gov). The drug is a potent inhibitor of BCR-Abl, Flt3, FGFR1 (Flt2), Kit, Src, VEGFR2, and PDGFRα/β (ChEMBL ID: CHEMBL1171837). We lack the X-ray crystal structure of the drug bound to Flt3, but we have the structure of the drug bound to the closely related Kit (PDB ID: 4u0i) [84]. This structure shows that the antagonist makes five hydrogen bonds with Kit. The *N*1 of the imidazopyridazine ring forms a hydrogen bond with the backbone amide group of the third hinge residue (C673), the amino group N−H forms a hydrogen bond with αC-E640, the benzamide carbonyl group hydrogen bonds with the N−H group of DFG-D810, and the piperazine N−H group forms bidentate hydrogen

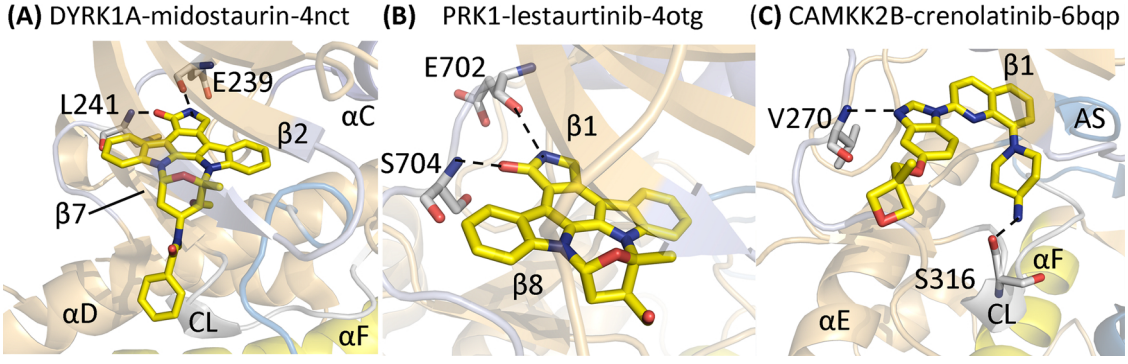

Fig. 8. Structures of drug-enzyme complexes. The dashed lines depict hydrogen bonds.

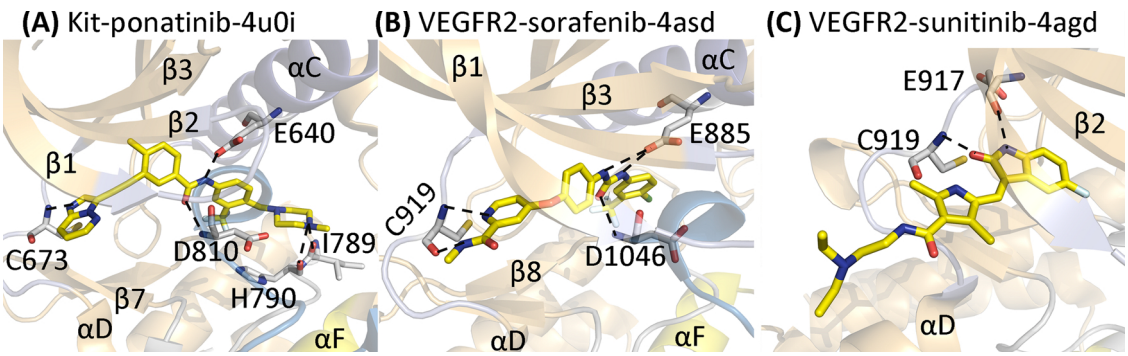

Fig. 9. Structures of drug-enzyme complexes. The dashed lines depict hydrogen bonds.

bonds with the carbonyl groups of I789 and H790 (RS1) (Fig. 9A). Ponatinib interacts hydrophobically with six spine residues (RS1/2/3, CS6/7/8), three shell residues (Sh1/2/3), and the KLIFS-3 residue. The drug also makes hydrophobic contact with residues near the ceiling of the adenine pocket including the β3-strand V622 and AVK-K623. The antagonist makes similar contact with E640, V643, L644 within the αC-helix, L647 and I653 in the back loop, V668 in the β5-strand, and E671,Y672 (the second hinge residue), and C673. The linear triple bond allows ponatinib to extend past the gatekeeper T670 into the back pocket. Ponatinib makes hydrophobic contact with C788, I789, and R791 within the catalytic loop and I808 within the β8-strand, C809 (the x of xDFG), and DFG-D810.

The drug binds to the front pocket, gate area, and back pockets including the BP-I-A/I-B, BP-II-out, and BP-III/IV. Ponatinib binds to the DFG-D_{out} conformation extending into the back pocket of Kit and is thereby classified as a type IIA inhibitor [52]. It is likely that ponatinib binds to Flt3 in a similar manner, but this remains to be established experimentally. Ponatinib is a multikinase inhibitor with activity against *FLT3*-mutants including ITD and ITD691L but not D835 within the Flt3 activation segment. This therapeutic is currently being used off label for AML patients [85].

Sorafenib is a diaryl-urea derivative (Fig. 6H) and multikinase inhibitor that is FDA-approved for the first-line treatment of hepatocellular and renal cell carcinomas and as a second-line treatment of radioiodine-refractory differentiated follicular and papillary thyroid carcinomas (Supplementary material). This medication was initially developed as a Raf protein-serine/threonine kinase inhibitor (B/C-Raf, B-Raf (V600E)), but it is also a potent antagonist of several receptor protein kinases including PDGFRα/β, Kit, Flt3, RET, and VEGFR1/2/3 [86–88]. The drug is a potent inhibitor of Flt3 bearing ITD mutations, but not activation segment mutations such as D835Y. The drug is in 38 clinical trials targeting AML (ClinicalTrials.gov). Numerous clinical trials indicate that sorafenib significantly improves the outcome when used as maintenance therapy after allo-hematopoietic stem cell transplantation; these studies have led to the off-label use for this condition [82,89]. This therapeutic is also used in combination with hypomethylating agents (azacitidine or decitabine) [17,18] in the off-label treatment of *FLT3*-mutated AML in patients unable to undergo cytotoxic chemotherapy.

We lack the X-ray crystal structure of sorafenib bound to Flt3, but we have the structure of the drug-VEGFR2 complex (4asd) [90]. The resulting pose shows that the antagonist makes five hydrogen bonds with VEGFR2. The terminal carboxamide N−H forms a hydrogen bond with the carbonyl group of C919 and the *N*1 of the pyrimidine forms a hydrogen bond with the N−H group of C919 (the third hinge residue). The two ureido N−H groups form hydrogen bonds with the carboxyl group of αC-E885 and the ureido carbonyl group forms a hydrogen bond with the N−H group of DFG-D1046 (Fig. 9B). The drug makes hydrophobic contact with six spine residues (RS1/2/3 and CS6/7/8), two shell residues (Sh1/2), and the KLIFS-3 residue. Moreover, the drug interacts hydrophobically with AVK-K868 as well as E885, I888, L889 within the αC-helix, I892 and V898 within the back loop, E917, F918, L919, K920 of the hinge-linker segment, I1044 of the β8-strand, C1045 (the x of xDFG), and DFG-D1046. Sorafenib binds in the front pocket, the gate area, back pocket, BP-I-B, BP-II-out, and BP-III. Sorafenib extends into the back pocket of the DFG-D_{out} conformation of VEGFR2 and is thereby classified as a type IIA inhibitor [52]. It is likely that sorafenib binds to Flt3 in a similar fashion, but this must be confirmed experimentally.

Sunitinib is an indole pyrrole (Fig. 6I) multikinase inhibitor that is FDA-approved for the first-line treatment of renal cell carcinoma and pancreatic neuroendocrine tumors and the second-line treatment of GIST (following initial imatinib therapy). This medication was developed as an anti-angiogenesis drug and inhibits Kit, PDGFα/β, MCSFR, LCK, and VEGFR1/2 as well as Flt3 [91–93]. The drug is or has been in seven clinical trials targeting AML (ClinicalTrials.gov); three of these trials are currently actively recruiting patients (February 2020). Fiedler et al. reported that 13 of 22 patients with AML treated with sunitinib had positive outcomes and achieved a complete response [94]. Whether or not the results of ongoing clinical trials will result in its approval by health authorities for the care of AML patients remains to be established.

We lack the X-ray crystal structure of sunitinib bound to Flt3, but we have the structure of the drug bound to the related VEGFR2 (4 agd) [90]. This structure shows that the N−H of its indole group amide forms a hydrogen bond with the carbonyl group of E917 (the first hinge residue) and the drug amide N−H group forms a hydrogen bond with the carbonyl group of C919 (the third hinge residue) (Fig. 9C). This interaction mimics the binding of the adenine base of ATP with protein kinases. The drug makes hydrophobic contact with four spine residues (RS2, CS6/7/8), two shell residues (Sh1/2), and KLIFS-3. The antagonist also interacts hydrophobically with AVK-K868 of the β3-strand, F918, C919, and K920 of the hinge-linker segment, C1045 (the x of xDFG), and DFG-D1046. The diethylaminoethyl group extends into the solvent. The drug interacts with the front pocket and BP-I-B. Sunitinib binds to the DFG-D_{out} conformation and does not extend past the gate area and is thereby classified as a type IIB inhibitor.

To summarize this section, the nine drugs form a hydrogen bond with the third hinge residue of their target enzyme and they interact hydrophobically with CS6/7/8 and the KLIFS-3 residue as well as the x of xDFG. These drugs also interact hydrophobically with one or more hinge-linker segment residues. Gilteritinib, sunitinib, midostaurin and lestaurtinib form a hydrogen bond with the first hinge residue. Quizartinib, crenolanib, ponatinib, and sorafenib bind to the DFG-D_{out} conformation and extend into the back pocket and are classified as type IIA inhibitors [52]. Midostaurin and lestaurtinib bind to the active form of their target enzyme and are classified as type I inhibitors. Gilteritinib and sunitinib bind to the DFG-D_{out} enzyme, but do not extend into the back pocket and are classified as type IIB inhibitors. Because these two therapeutics do not extend into the back pocket, these compounds may also function as type I inhibitors.

6. Analyses of the chemical properties of orally effective drugs

6.1. Lipinski's rule of five (Ro5)

Medicinal chemists and pharmacologists have searched for beneficial drug-like chemical properties that result in medicines with oral therapeutic effectiveness. Lipinski's "rule of five" is an experimental and computational methodology to estimate membrane permeability, solubility, and effectiveness in the drug-development setting [95]. It is a rule of thumb that evaluates drug-likeness and determines whether a compound with particular pharmacological activities has physical and chemical properties that indicate it would make an effective drug when given orally. The Lipinski factors were based upon the observation that most orally effective medicinals are small and moderately lipophilic molecules. The Ro5 criteria are used during drug discovery when pharmacologically active prototype molecules are serially optimized to increase their activity and selectivity while maintaining their drug-like physicochemical characteristics.

The Ro5 hypothesizes that less than ideal oral efficacy is more likely to be found when (i) the calculated Log P (cLogP) is greater than 5, when (ii) there are more than 5 hydrogen-bond donors, when (iii) there are more than 5 × 2 or 10 hydrogen-bond acceptors, and when (iv) the molecular weight is greater than 5 × 100 or 500 [95]. The partition coefficient (P) is the ratio of the concentration of the un-ionized compound in the organic phase of water-saturated *n*-octanol divided by its concentration in the aqueous phase. The P value is a surrogate of hydrophobicity; the larger the P value, the greater the hydrophobicity. The tally of hydrogen-bond donors is the sum of OH and NH groups and that of hydrogen-bond acceptors consists of heteroatoms lacking a formal positive charge apart from halogen atoms, pyrrole nitrogen atoms, heteroaromatic sulfur and oxygen atoms, and higher oxidation states of nitrogen, sulfur, and phosphorus, but including the oxygen atoms bonded to them. The Ro5 criteria are based upon the chemical characteristics of more than two thousand reference drugs [95].

6.2. Additional chemical descriptors of druglike properties

The Ro5 has generated many corollaries to improve oral effectiveness. For example, Veber et al. reported that the polar surface area (PSA) and the number of rotatable bonds differentiates between orally active and inactive drugs for a large series of substances in rats [96]. These investigators found that compounds with polar surface area values less than or equal to 140 $Å^2$ exhibit effective oral bioavailability. The PSA is the sum of the surface over all polar atoms, primarily oxygen and nitrogen, but also including their associated hydrogen atoms. The nine Flt3 inhibitors covered in this section have a polar surface area less than 140 $Å^2$ (Table 5). Furthermore, these investigators concluded that the optimal number of rotatable bonds is less than or equal to 10. Rotatable bonds are associated with molecular flexibility (degrees of freedom) and are regarded as an important factor in passive membrane permeation. Except for FF10101, which has 14 rotatable bonds, the other drugs have 9 or fewer rotatable bonds. Moreover, Oprea observed that the number of rings in most orally approved drugs is three or more [97]. All the drugs considered in this section have three or more rings with the exception again of FF10101.

The molecular complexity of a drug is based upon its structural features, symmetry, and the elements it contains. This parameter is computed with the Bertz/Hendrickson algorithm [98,99]. It is based upon the nature of the chemical bonds, their bonding pattern, and their identity. The molecular complexity ranges from 0 (simple ions) to several thousand (complex natural products). All of the molecular complexity values for the drugs in Table 5 were obtained from PubChem (https://pubchem.ncbi.nlm.nih.gov/). There are no established or optimal molecular complexity values for orally effective drugs. However, the data show that midostaurin has the highest value for the Flt3 inhibitors covered in this review.

7. Epilogue

Although the mode of binding or pose of each medicinal with its protein kinase target is unique, it is useful to generalize drug-enzyme interactions and employ them in the drug development and discovery process. We divided protein kinase inhibitors into seven possible types (I–VI and I½) based upon the nature of their drug-enzyme complexes [52]. The complexity of inhibitor taxonomy increases because some medications can bind to different conformations of their protein kinase targets. For example, crizotinib is a type I inhibitor of ALK and a type I½B inhibitor of c-Met (both are receptor protein-tyrosine kinases). Moreover, bosutinib is a type I antagonist of Src and a type IIB antagonist of the Abl (both are non-receptor protein-tyrosine kinases). Additionally, sunitinib is a type I½B inhibitor of CDK2 (cyclin-dependent protein kinase 2, a protein-serine/threonine kinase) and a type IIB inhibitor of Kit (a receptor protein-tyrosine kinase). Furthering this complexity, the X-ray crystal structures demonstrate that erlotinib can be a type I or I½B inhibitor of EGFR/ErbB1 (a receptor protein-tyrosine kinase). These data indicate that some protein kinase blockers lack conformational selectivity. Surprisingly, the prototypical classical type IIA inhibitor imatinib [52] was observed to bind to the active non-receptor Syk protein-tyrosine kinase with αC_{in} and an open DFG-D_{in} activation segment as a type I inhibitor (PDB ID: 1xbb) [100]. In this case, imatinib assumes a compact U-shaped structure that occurs only within the front pocket, which contrasts with its binding to Abl in an extended linear conformation (PDB ID: 2hyy) [101].

As indicated in Table 4, all the drugs reviewed in this paper target several enzymes. Carles et al. prepared a comprehensive catalog of more than 175 orally effective small molecule protein kinase and phosphatidyl inositol-3 kinase inhibitors that are or have been in clinical trials [102]. They created a non-commercial and searchable web site, which is also regularly updated, that includes physicochemical structures and properties of various inhibitors, their protein targets, their therapeutic indications, the year of first approval (if applicable), and their trade names (http://www.icoa.fr/pkidb/). Furthermore, the BRIMR (Blue Ridge Institute for Medical Research) website, which is also regularly updated, depicts the structures and the Lipinski rule of five properties [95] of all small molecule protein kinase inhibitors that have been approved by the US FDA (www.brimr.org/PKI/PKIs.htm).

Although one goal in drug discovery and development of protein kinase antagonists has been to inhibit a single enzyme, it appears that many, if not most, of so-called selective inhibitors have been found at later stages to inhibit multiple enzymes. It appears that most FDA-approved protein kinase antagonists are multikinase inhibitors. This has potential advantages as well as drawbacks. It is conceivable that the therapeutic efficacy of multikinase inhibitors may be related to the inhibition of more than one enzyme. For example, sunitinib and cabozantinib have potent Axl off-target activity and this property may add to their clinical efficacy [103]. Contrariwise, the inhibition of off-target enzymes may produce adverse side effects. Consequently, we have the problem of whether magic shotguns are to be preferred over magic bullets [104].

The US FDA approved imatinib for the treatment of chronic myelogenous leukemia in 2001 and this approval ushered in the use of small molecule protein kinase inhibitors for various cancers and inflammatory diseases [2]. Imatinib inhibits the BCR-Abl protein kinase oncoprotein that results from the formation of the Philadelphia chromosome. Nearly fifty other orally effective small molecule protein kinase inhibitors have been subsequently approved by the FDA for the treatment of various neoplasms. Resistance to nearly all the FDA-approved protein kinase inhibitors occurs within several months to a few years. Moreover, most of these protein kinase inhibitors prolong survival in cancer patients only weeks or months longer than standard cytotoxic therapies.

In contrast, the clinical effectiveness of imatinib against chronic myelogenous leukemia is vastly superior to that of any other small

Table 5
Properties of selected Flt3 small molecule inhibitors[a].

Drug	PubMED CID	Formula	MW (Da)	HD [b]	HA [c]	cLogP [a,d]	Rotatable bonds	PSA[e] (Å^2)	Ring count	Complexity [f]
Gilteritinib	49803313	$C_{29}H_{44}N_8O_3$	553	3	10	3.0	9	121	5	785
Quizartinib	24889392	$C_{29}H_{32}N_6O_4S$	561	2	8	5.48	8	134	5	849
FF10101	90052320	$C_{29}H_{38}N_8O_2$	531	3	8	3.12	14	126	2	906
Midostaurin	9829523	$C_{35}H_{30}N_4O_4$	571	1	4	5.3	3	77.7	7	1140
Lestaurtinib	126565	$C_{26}H_{21}N_3O_4$	439	3	4	2.82	1	88.6	7	886
Crenolanib	10366136	$C_{26}H_{29}N_5O_2$	443	1	6	3.79	5	78.4	6	667
Ponatinib	24826799	$C_{29}H_{27}F_3N_6O$	533	1	8	4.7	6	65.8	5	910
Sorafenib	216239	$C_{21}H_{16}ClF_3N_4O_3$	465	3	7	3.2	5	92.4	3	646
Sunitinib	5329102	$C_{22}H_{27}FN_4O_2$	399	3	4	3.02	7	77.2	3	636

[a] All data from NIH PubChem except for cLogP (the calculated Log_{10} of the partition coefficient, which was computed using MedChem Designer™, version 2.0, Simulationsplus, Inc. Lancaster, CA 93534.
[b] No. of hydrogen bond donors.
[c] No. of hydrogen bond acceptors.
[d] Calculated Log_{10} of the partition coefficient.
[e] (PSA) Polar surface area.
[f] Values obtained from https://pubchem.ncbi.nlm.nih.gov/.

molecule protein kinase inhibitor with overall survival rates lasting a decade or more. For example, Hochhaus et al. reported that the overall 10-year survival rate was 83 % in those people who received the drug [105]. Moreover, Molica et al. reported that imatinib maintains its efficacy over time and long-term administration is not associated with late term toxic effects [106]. Such long-term benefits in the treatment of CML with imatinib are truly unique among small molecule protein kinase inhibitors and the drug represents, in the words of Paul Ehrlich, a magic bullet. One reason for the effectiveness of imatinib in the treatment of CML is that the disease is driven solely by the formation of BCR-Abl as a result of the formation of the Philadelphia chromosome whereas nearly all other malignancies such as AML are the result of multiple driving factors [2]. Owing to the multiplicity of signaling aberrations that produce AML, it is not surprising that administration of Flt3 antagonists, even in patients with *FLT3* mutations, is not more efficacious.

The Flt3 signaling family includes only Flt3L and its receptor Flt3 which parallels the stem cell factor (SCF) and its Kit receptor. In contrast, the PDGFR family involves four growth factors and two receptors (Table 6). Five growth factors and three receptors make up the VEGFR family and 11 growth factors and four receptors make up the ErbB family. The FGF family is one of the largest, if not the largest, signaling constellation which is made up of a total of 22 growth factors, four protein-tyrosine kinase receptors, and a fifth receptor lacking intracellular enzyme activity. The potential combinatorial interactions of FGF1–23 and FGFR1–4 numbers in the thousands. This multiplicity increases the difficulty in deciphering specific signaling pathways. In principle, deciphering the Flt3 and Kit signal transduction pathways is easier than those of the other growth factor receptors, but untangling the signaling mechanisms of these two pathways has not been easy [8,107].

Manning et al. reported that the human protein kinase super family consists of 518 members [4]. If the number of human genes is about 19,000 [108], then protein kinases make up 2.7 % of all genes. Thus, about 1 in 37 genes encodes a protein kinase. Because mutations and dysregulation of protein kinases play fundamental roles in the pathogenesis of human diseases including autoimmune, inflammatory, and nervous disorders as well as cancer, this family of enzymes has become one of the most important drug targets over the past two decades [1,2]. There are 55 FDA-approved medications that are directed against about 20 different protein kinases (Supplementary material) and drugs targeting an additional 20 protein kinases are in clinical trials worldwide [102]. For a review of the properties of 53 of the 55 approved drugs, see Refs. [109,110]. Owing to the hundreds of disease loci or cancer amplicons that have been mapped in the human genome [4], one can anticipate a substantial increase in the number of enzymes that will be targeted for the treatment of more and more illnesses.

Table 6
Growth factor families.

Growth factor receptors	Growth factors/ligands
Flt3 [8]	Flt3L
Kit [107]	Stem cell factor (SCF)
PDGFRα/β [46]	PDGF-A/B/C/D
VEGFR1/2/3 [49]	VEGF-A/B/C/D, placental growth factor (PlGF)
ErbB1/2/3/4 [41,42] [a]	EGF, epigen (EPG), transforming growth factor-α (TGF-α), amphiregulin (AR), betacellulin (BTC), heparin-binding epidermal growth-factor like growth factor (HB-EGF), epiregulin (EPR), neuregulin-1/2/3/4 (Nrg-1/2/3/4)
FGFR1-IIIB & IIIC/FGFR2-IIIB & IIIC/FGFR3-IIIB & IIIC/FGFR4/FGFRL1 [50]	22 FGF gene products

[a] Members of the epidermal growth factor receptor (EGFR) family.

Declaration of Competing Interest

The author is unaware of any affiliations, memberships, or financial holdings that might be perceived as affecting the objectivity of this review.

Acknowledgments

The colored figures in this paper were checked to ensure that their perception was accurately conveyed to colorblind readers [111]. The author thanks Laura M. Roskoski for providing editorial and bibliographic assistance. I also thank Josie Rudnicki and Jasper Martinsek help in preparing the figures and Pasha Brezina and W.S. Sheppard for their help in structural analyses.

Appendix A. Supplementary data

Supplementary material related to this article can be found, in the online version, at doi:https://doi.org/10.1016/j.phrs.2020.104725.

References

[1] P. Cohen, Protein kinases – the major drug targets of the twenty-first century? Nat. Rev. Drug Discov. 1 (2002) 309–315.
[2] R. Roskoski Jr., A historical overview of protein kinases and their targeted small

molecule inhibitors, Pharmacol. Res. 100 (2015) 1–23.
[3] P.M. Fischer, Approved and experimental small-molecule oncology kinase inhibitor drugs: a mid-2016 overview, Med. Res. Rev. 37 (2017) 314–367.
[4] G. Manning, D.B. Whyte, R. Martinez, T. Hunter, S. Sudarsanam, The protein kinase complement of the human genome, Science 298 (2002) 1912–1934.
[5] A. Alonso, R. Pulido, The extended human PTPome: a growing tyrosine phosphatase family, FEBS J. 283 (2016) 1404–1429 Erratum in: FEBS J 2016;283:2197–201.
[6] S.K. McDonough, S. Larsen, R.S. Brodey, N.D. Stock, W.D. Hardy Jr., A transmissible feline fibrosarcoma of viral origin, Cancer Res. 31 (1971) 953–956.
[7] D.L. Stirewalt, J.P. Radich, The role of FLT3 in haematopoietic malignancies, Nat. Rev. Cancer 3 (2003) 650–665.
[8] J.U. Kazi, L. Rönnstrand, FMS-like tyrosine kinase 3/FLT3: from basic science to clinical implications, Physiol. Rev. 99 (2019) 1433–1466.
[9] C.C. Coombs, M.S. Tallman, R.L. Levine, Molecular therapy for acute myeloid leukaemia, Nat. Rev. Clin. Oncol. 13 (2016) 305–318.
[10] C. Thiede, C. Steudel, B. Mohr, M. Schaich, U. Schäkel, U. Platzbecker, et al., Analysis of FLT3-activating mutations in 979 patients with acute myelogenous leukemia: association with FAB subtypes and identification of subgroups with poor prognosis, Blood 99 (2002) 4326–4335.
[11] M.M. Patnaik, The importance of *FLT3* mutational analysis in acute myeloid leukemia, Leuk. Lymphoma 59 (2018) 2273–2286.
[12] W.J. Fantl, D.E. Johnson, L.T. Williams, Signaling by receptor tyrosine kinases, Annu. Rev. Biochem. 62 (1993) 453–481.
[13] M.A. Lemmon, J. Schlessinger, Cell signaling by receptor tyrosine kinases, Cell 141 (2010) 1117–1134.
[14] S.N. Savvides, T. Boone, P. Andrew Karplus, Flt3 ligand structure and unexpected commonalities of helical bundles and cystine knots, Nat. Struct. Biol. 7 (2000) 486–491.
[15] K. Verstraete, G. Vandriessche, M. Januar, J. Elegheert, A.V. Shkumatov, A. Desfosses, et al., Structure insights into the extracellular assembly of the hematopoietic Flt3 signaling complex, Blood 118 (2011) 60–80.
[16] R.L. Siegel, K.D. Miller, A. Jemal, Cancer statistics, 2020, CA Cancer J. Clin. 70 (2020) 7–30.
[17] J.G. Herman, S.B. Baylin, Gene silencing in cancer in association with promoter hypermethylation, N. Engl. J. Med. 349 (2003) 2042–2054.
[18] J. Diesch, A. Zwick, A.K. Garz, A. Palau, M. Buschbeck, K.S. Götze, A clinical-molecular update on azanucleoside-based therapy for the treatment of hematologic cancers, Clin. Epigenetics 8 (2016) 71.
[19] L.E. Locascio, D.J. Donoghue, KIDs rule: regulatory phosphorylation of RTKs, Trends Biochem. Sci. 38 (2013) 75–84.
[20] S.K. Hanks, T. Hunter, Protein kinases 6. The eukaryotic protein kinase superfamily: kinase (catalytic) domain structure and classification, FASEB J. 9 (1995) 576–596.
[21] D.R. Knighton, J.H. Zheng, L.F. Ten Eyck, V.A. Ashford, N.H. Xuong, S.S. Taylor, et al., Crystal structure of the catalytic subunit of cyclic adenosine monophosphate-dependent protein kinase, Science 253 (1991) 407–414.
[22] D.R. Knighton, J.H. Zheng, L.F. Ten Eyck, N.H. Xuong, S.S. Taylor, J.M. Sowadski, Structure of a peptide inhibitor bound to the catalytic subunit of cyclic adenosine monophosphate-dependent protein kinase, Science 253 (1991) 414–420.
[23] R. Roskoski Jr., Src protein-tyrosine kinase structure, mechanism, and small molecule inhibitors, Pharmacol. Res. 94 (2015) 9–25.
[24] A.C. Bastidas, M.S. Deal, J.M. Steichen, Y. Guo, J. Wu, S.S. Taylor, Phosphoryl transfer by protein kinase A is captured in a crystal lattice, J. Am. Chem. Soc. 135 (2013) 4788–4798.
[25] S.S. Taylor, M.M. Keshwani, J.M. Steichen, A.P. Kornev, Evolution of the eukaryotic protein kinases as dynamic molecular switches, Philos. Trans. R. Soc. Lond. B Biol. Sci. 367 (2012) 2517–2528.
[26] B. Nolen, S. Taylor, G. Ghosh, Regulation of protein kinases; controlling activity through activation segment conformation, Mol. Cell 15 (2004) 661–675.
[27] D.J. Rawlings, A.M. Scharenberg, H. Park, M.I. Wahl, S. Lin, R.M. Kato, et al., Activation of BTK by a phosphorylation mechanism initiated by SRC family kinases, Science 271 (1996) 822–825.
[28] H. Chen, J. Ma, W. Li, A.V. Eliseenkova, C. Xu, T.A. Neubert, et al., A molecular brake in the kinase hinge region regulates the activity of receptor tyrosine kinases, Mol. Cell 27 (2007) 717–730.
[29] J. Zhou, J.A. Adams, Participation of ADP dissociation in the rate-determining step in cAMP-dependent protein kinase, Biochemistry 36 (1997) 15733–15738.
[30] A.P. Kornev, N.M. Haste, S.S. Taylor, L.F. Ten Eyck, Surface comparison of active and inactive protein kinases identifies a conserved activation mechanism, Proc. Natl. Acad. Sci. U. S. A. 103 (2006) 17783–17788.
[31] A.P. Kornev, S.S. Taylor, L.F. Ten Eyck, A helix scaffold for the assembly of active protein kinases, Proc. Natl. Acad. Sci. U. S. A. 105 (2008) 14377–14382.
[32] R. Roskoski Jr., Anaplastic lymphoma kinase (ALK): structure, oncogenic activation, and pharmacological inhibition, Pharmacol. Res. 68 (2013) 68–94.
[33] R. Roskoski Jr., Anaplastic lymphoma kinase (ALK) inhibitors in the treatment of ALK-driven lung cancers, Pharmacol. Res. 117 (2017) 343–356.
[34] R. Roskoski Jr., Targeting oncogenic Raf protein-serine/threonine kinases in human cancers, Pharmacol. Res. 135 (2018) 239–258.
[35] R. Roskoski Jr., RAF protein-serine/threonine kinases: structure and regulation, Biochem. Biophys. Res. Commun. 399 (2010) 313–317.
[36] R. Roskoski Jr., Ibrutinib inhibition of Bruton protein-tyrosine kinase (BTK) in the treatment of B cell neoplasms, Pharmacol. Res. 113 (2016) 395–408.
[37] R. Roskoski Jr., Cyclin-dependent protein kinase inhibitors including palbociclib as anticancer drugs, Pharmacol. Res. 111 (2016) 784–803.
[38] R. Roskoski Jr., Cyclin-dependent protein serine/threonine kinase inhibitors as anticancer drugs, Pharmacol. Res. 139 (2019) 471–488.
[39] R. Roskoski Jr., ERK1/2 MAP kinases: structure, function, and regulation, Pharmacol. Res. 66 (2012) 105–143.
[40] R. Roskoski Jr., Targeting ERK1/2 protein-serine/threonine kinases in human cancers, Pharmacol. Res. 142 (2019) 151–168.
[41] R. Roskoski Jr., ErbB/HER protein-tyrosine kinases: structures and small molecule inhibitors, Pharmacol. Res. 79 (2014) 34–74.
[42] R. Roskoski Jr., Small molecule inhibitors targeting the EGFR/ErbB family of protein-tyrosine kinases in human cancers, Pharmacol. Res. 139 (2019) 395–411.
[43] R. Roskoski Jr., Janus kinase (JAK) inhibitors in the treatment of inflammatory and neoplastic diseases, Pharmacol. Res. 111 (2016) 784–803.
[44] R. Roskoski Jr., MEK1/2 dual-specificity protein kinases: structure and regulation, Biochem. Biophys. Res. Commun. 417 (2012) 5–10.
[45] R. Roskoski Jr., Allosteric MEK1/2 inhibitors including cobimetanib and trametinib in the treatment of cutaneous melanomas, Pharmacol. Res. 117 (2017) 20–31.
[46] R. Roskoski Jr., The role of small molecule platelet-derived growth factor receptor (PDGFR) inhibitors in the treatment of neoplastic disorders, Pharmacol. Res. 129 (2018) 65–83.
[47] R. Roskoski Jr., A. Sadeghi-Nejad, Role of RET protein-tyrosine kinase inhibitors in the treatment RET-driven thyroid and lung cancers, Pharmacol. Res. 128 (2018) 1–17.
[48] R. Roskoski Jr., ROS1 protein-tyrosine kinase inhibitors in the treatment of ROS1 fusion protein-driven non-small cell lung cancers, Pharmacol. Res. 121 (2017) 202–212.
[49] R. Roskoski Jr., Vascular endothelial growth factor (VEGF) and VEGF receptor inhibitors in the treatment of renal cell carcinomas, Pharmacol. Res. 120 (2017) 116–132.
[50] R. Roskoski Jr., The role of fibroblast growth factor receptor (FGFR) protein-tyrosine kinase inhibitors in the treatment of cancers including those of the urinary bladder, Pharmacol. Res. 151 (2020) 104567.
[51] H.S. Meharena, P. Chang, M.M. Keshwani, K. Oruganty, A.K. Nene, N. Kannan, et al., Deciphering the structural basis of eukaryotic protein kinase regulation, PLoS Biol. 11 (2013) e1001690.
[52] R. Roskoski Jr., Classification of small molecule protein kinase inhibitors based upon the structures of their drug-enzyme complexes, Pharmacol. Res. 103 (2016) 26–48.
[53] K. Shah, Y. Liu, C. Deirmengian, K.M. Shokat, Engineering unnatural nucleotide specificity for Rous sarcoma virus tyrosine kinase to uniquely label its direct substrates, Proc. Natl. Acad. Sci. U. S. A. 94 (1997) 3565–3570.
[54] Y. Liu, K. Shah, F. Yang, L. Witucki, K.M. Shokat, A molecular gate which controls unnatural ATP analogue recognition by the tyrosine kinase v-Src, Bioorg. Med. Chem. 6 (1998) 1219–1226.
[55] J.J. Liao, Molecular recognition of protein kinase binding pockets for design of potent and selective kinase inhibitors, J. Med. Chem. 50 (2007) 409–424.
[56] A.C. Dar, K.M. Shokat, The evolution of protein kinase inhibitors from antagonists to agonists of cellular signaling, Annu. Rev. Biochem. 80 (2011) 769–795.
[57] F. Zuccotto, E. Ardini, E. Casale, M. Angiolini, Through the "gatekeeper door": exploiting the active kinase conformation, J. Med. Chem. 53 (2010) 2691–2694.
[58] L.K. Gavrin, E. Saiah, Approaches to discover non-ATP site inhibitors, Med. Chem. Res. 4 (2013) 41.
[59] V. Lamba, I. Ghosh, New directions in targeting protein kinases: focusing upon true allosteric and bivalent inhibitors, Curr. Pharm. Des. 18 (2012) 2936–2945.
[60] T.K. Johnson, M.B. Soellner, Bivalent inhibitors of c-Src tyrosine kinase that bind a regulatory domain, Bioconjug. Chem. 27 (2016) 1745–1749.
[61] R.A. Copeland, The drug-target residence time model: a 10-year retrospective, Nat. Rev. Drug Discov. 15 (2016) 87–95.
[62] O.P. van Linden, A.J. Kooistra, R. Leurs, I.J. de Esch, C. de Graaf, KLIFS: a knowledge-based structural database to navigate kinase-ligand interaction space, J. Med. Chem. 57 (2014) 249–277.
[63] A.J. Kooistra, A. Volkamer, Kinase-centric computational drug development, Ann. Rep. Med. Chem. 50 (2017) 197–236.
[64] D. Bajusz, G.G. Ferenczy, G.M. Keserá, Structure-based virtual screening approaches in kinase-directed drug discovery, Curr. Top. Med. Chem. 17 (2017) 2235–2259.
[65] P. Wu, T.E. Nielsen, M.H. Clausen, FDA-approved small-molecule kinase inhibitors, Trends Pharmacol. Sci. 36 (2015) 422–439.
[66] G.K. Kanev, C. de Graaf, I.J.P. de Esch, R. Leurs, T. Würdinger, B.A. Westerman, et al., The landscape of atypical and eukaryotic protein kinases, Trends Pharmacol. Sci. 40 (2019) 818–832.
[67] S. Dhillon, Gilteritinib: First global approval, Drugs 79 (2019) 331–339.
[68] H. Kiyoi, N. Kawashima, Y. Ishikawa, *FLT3* mutations in acute myeloid leukemia: therapeutic paradigm beyond inhibitor development, Cancer Sci. 111 (2) (2020) 312–322, https://doi.org/10.1111/cas.14274.
[69] N.J. Short, H. Kantarjian, F. Ravandi, N. Daver, Emerging treatment paradigms with FLT3 inhibitors in acute myeloid leukemia, Ther. Adv. Hematol. 10 (2019) 2040620719827310.
[70] T. Yamaura, T. Nakatani, K. Uda, H. Ogura, W. Shin, N. Kurokawa, et al., A novel irreversible FLT3 inhibitor, FF-10101, shows excellent efficacy against AML cells with *FLT3* mutations, Blood 131 (2018) 426–438.
[71] T. Meyer, U. Regenass, D. Fabbro, E. Alteri, J. Rösel, M. Müller, et al., A derivative of staurosporine (CGP 41 251) shows selectivity for protein kinase C inhibition and *in vitro* anti-proliferative as well as *in vivo* anti-tumor activity, Int. J. Cancer 43 (1989) 851–856.
[72] E. Weisberg, C. Boulton, L.M. Kelly, P. Manley, D. Fabbro, T. Meyer, et al., Inhibition of mutant FLT3 receptors in leukemia cells by the small molecule

tyrosine kinase inhibitor PKC412, Cancer Cell 1 (2002) 433–443.
[73] J. Gotlib, H.C. Kluin-Nelemans, T.I. George, C. Akin, K. Sotlar, O. Hermine, et al., Efficacy and safety of midostaurin in advanced systemic mastocytosis, N. Engl. J. Med. 374 (2016) 2530–2541.
[74] D.J. DeAngelo, T.I. George, A. Linder, C. Langford, C. Perkins, J. Ma, et al., Efficacy and safety of midostaurin in patients with advanced systemic mastocytosis: 10-year median follow-up of a phase II trial, Leukemia 32 (2018) 470–478.
[75] R.M. Stone, P.W. Manley, R.A. Larson, R. Capdeville, Midostaurin: its odyssey from discovery to approval for treating acute myeloid leukemia and advanced systemic mastocytosis, Blood Adv. 2 (2018) 444–453.
[76] J.D. Growney, J.J. Clark, J. Adelsperger, R. Stone, D. Fabbro, J.D. Griffin, et al., Activation mutations of human c-KIT resistant to imatinib mesylate are sensitive to the tyrosine kinase inhibitor PKC412, Blood 106 (2005) 721–724.
[77] M. Alexeeva, E. Åberg, R.A. Engh, U. Rothweiler, The structure of a dual-specificity tyrosine phosphorylation-regulated kinase 1A-PKC412 complex reveals disulfide-bridge formation with the anomalous catalytic loop HRD(HCD) cysteine, Acta Crystallogr. D Biol. Crystallogr. 71 (2015) 1207–1215.
[78] D.J. George, C.A. Dionne, J. Jani, T. Angeles, C. Murakata, J. Lamb, et al., Sustained *in vivo* regression of Dunning H rat prostate cancers treated with combinations of androgen ablation and Trk tyrosine kinase inhibitors, CEP-751 (KT-6587) or CEP-701 (KT-5555), Cancer Res. 59 (1999) 2395–2401.
[79] M. Levis, J. Allebach, K.F. Tse, R. Zheng, B.R. Baldwin, B.D. Smith, et al., A FLT3-targeted tyrosine kinase inhibitor is cytotoxic to leukemia cells in vitro and in vivo, Blood 99 (2002) 3885–3891.
[80] P. Chamberlain, S. Delker, B. Pagarigan, A. Mahmoudi, P. Jackson, M. Abbasian, et al., Crystal structures of PRK1 in complex with the clinical compounds lestaurtinib and tofacitinib reveal ligand induced conformational changes, PLoS One 9 (2014) e103638.
[81] S. Knapper, N. Russell, A. Gilkes, R.K. Hills, R.E. Gale, J.D. Cavenagh, et al., A randomized assessment of adding the kinase inhibitor lestaurtinib to first-line chemotherapy for FLT3-mutated AML, Blood 129 (2017) 1143–1154.
[82] A.I. Antar, Z.K. Otrock, E. Jabbour, M. Mohty, A. Bazarbachi, FLT3 inhibitors in acute myeloid leukemia: ten frequently asked questions, Leukemia (2020), https://doi.org/10.1038/s41375-019-0694-3.
[83] G.S. Profeta, C.V. Dos Reis, A.D.S. Santiago, P.H.C. Godoi, A.M. Fala, C.I. Wells, et al., Binding and structural analyses of potent inhibitors of the human Ca^{2+}/calmodulin dependent protein kinase 2 (CAMKK2) identified from a collection of commercially-available kinase inhibitors, Sci. Rep. 9 (2019) 16452.
[84] A.P. Garner, J.M. Gozgit, R. Anjum, S. Vodala, A. Schrock, T. Zhou, et al., Ponatinib inhibits polyclonal drug-resistant KIT oncoproteins and shows therapeutic potential in heavily pretreated gastrointestinal stromal tumor (GIST) patients, Clin. Cancer Res. 20 (2014) 5745–5755.
[85] E.S. Wang, Beyond midostaurin: which are the most promising FLT3 inhibitors in AML? Best Pract. Res. Clin. Haematol. 32 (2019) 101103.
[86] S. Wilhelm, D.S. Chien, BAY 43-9006: preclinical data, Curr. Pharm. Des. 8 (2002) 2255–2257.
[87] D. Strumberg, Preclinical and clinical development of the ral multikinase inhibitor sorafenib in cancer treatment, Drugs Today (Barc) 41 (2005) 773–784.
[88] T. Guo, N.P. Agaram, G.C. Wong, G. Hom, D. D'Adamo, R.G. Maki, et al., Sorafenib inhibits the imatinib-resistant KITT670I gatekeeper mutation in gastrointestinal stromal tumor, Clin. Cancer Res. 13 (2007) 4874–4881.
[89] G. Chappell, M. Geer, E. Gatza, T. Braun, T. Churay, J. Brisson, et al., Maintenance sorafenib in FLT3-ITD AML following allogeneic HCT favorably impacts relapse and overall survival, Bone Marrow Transplant. 54 (2019) 1518–1520.
[90] M. McTigue, B.W. Murray, J.H. Chen, Y.L. Deng, J. Solowiej, R.S. Kania, Molecular conformations, interactions, and properties associated with drug efficiency and clinical performance among VEGFR TK inhibitors, Proc. Natl. Acad. Sci. U. S. A. 109 (2012) 18281–18289.
[91] A. Wozniak, Y.K. Gebreyohannes, M. Debiec-Rychter, P. Schöffski, New targets and therapies for gastrointestinal stromal tumors, Expert Rev. Anticancer Ther. 17 (2017) 1117–1129.
[92] R. Roskoski Jr., STI-571: an anticancer protein-tyrosine kinase inhibitor, Biochem. Biophys. Res. Commun. 309 (2003) 709–717.
[93] R. Roskoski Jr., Sunitinib: a VEGF and PDGF receptor protein kinase and angiogenesis inhibitor, Biochem. Biophys. Res. Commun. 356 (2007) 323–328.
[94] W. Fiedler, S. Kayser, M. Kebenko, M. Janning, J. Krauter, M. Schittenhelm, et al., A phase I/II study of sunitinib and intensive chemotherapy in patients over 60 years of age with acute myeloid leukaemia and activating *FLT3* mutations, Br. J. Haematol. 169 (2015) 694–700.
[95] C.A. Lipinski, F. Lombardo, B.W. Dominy, P.J. Feeney, Experimental and computational approaches to estimate solubility and permeability in drug discovery and development settings, Adv. Drug Deliv. Rev. 46 (2001) 3–26.
[96] D.F. Veber, S.R. Johnson, H.Y. Cheng, B.R. Smith, K.W. Ward, K.D. Kopple, Molecular properties that influence the oral bioavailability of drug candidates, J. Med. Chem. 45 (2002) 2615–2623.
[97] T.I. Oprea, Property distribution of drug-related chemical databases, J. Comput. Aided Mol. Des. 14 (2000) 251–264.
[98] S.H. Bertz, The first general index of molecular complexity, J. Am. Chem. Soc. 1103 (1981) 3559–3601.
[99] J.B. Hendrickson, P. Huang, A.G. Toczko, Molecular complexity: a simplified formula adapted to individual atoms, J. Chem. Inf. Comput. Sci. 27 (1987) 63–67.
[100] S. Atwell, J.M. Adams, J. Badger, M.D. Buchanan, I.K. Feil, K.J. Froning, et al., A novel mode of Gleevec binding is revealed by the structure of spleen tyrosine kinase, J. Biol. Chem. 279 (2004) 55827–55832.
[101] S.W. Cowan-Jacob, G. Fendrich, A. Floersheimer, P. Furet, J. Liebetanz, G. Rummel, et al., Structural biology contributions to the discovery of drugs to treat chronic myelogenous leukaemia, Acta Crystallogr. D Biol. Crystallogr. 63 (2007) 80–93.
[102] F. Carles, S. Bourg, C. Meyer, P. Bonnet, PKIDB: a curated, annotated and updated database of protein kinase inhibitors in clinical trials, Molecules 23 (2018) E908, https://doi.org/10.3390/molecules23040908.
[103] S.H. Myers, V.G. Brunton, A. Unciti-Broceta, AXL inhibitors in cancer: a medicinal chemistry perspective, J. Med. Chem. 59 (2016) 3593–3608.
[104] B.L. Roth, D.J. Sheffler, W.K. Kroeze, Magic shotguns versus magic bullets: selectively non-selective drugs for mood disorders and schizophrenia, Nat. Rev. Drug Discov. 3 (2004) 353–359.
[105] A. Hochhaus, R.A. Larson, F. Guilhot, J.P. Radich, S. Branford, T.P. Hughes, et al., Long-term outcomes of imatinib treatment for chronic myeloid leukemia, N. Engl. J. Med. 376 (2017) 917–927.
[106] M. Molica, G. Colafigli, E. Scalzulli, D. Alunni Fegatelli, S. Chiatamone Ranieri, L. Rizzo, et al., Ten-year outcome of chronic-phase chronic myeloid leukemia patients treated with imatinib in real life, Ann. Hematol. 98 (2019) 1891–1904.
[107] R. Roskoski Jr., The role of small molecule Kit protein-tyrosine kinase inhibitors in the treatment of neoplastic disorders, Pharmacol. Res. 133 (2018) 35–52.
[108] I. Ezkurdia, D. Juan, J.M. Rodriguez, A. Frankish, M. Diekhans, J. Harrow, et al., Multiple evidence strands suggest that there may be as few as 19,000 human protein-coding genes, Hum. Mol. Genet. 23 (2014) 5866B78.
[109] R. Roskoski Jr., Properties of FDA-approved small molecule protein kinase inhibitors, Pharmacol. Res. 144 (2019) 19–50.
[110] R. Roskoski Jr., Properties of FDA-approved small molecule protein kinase inhibitors: a 2020 update, Pharmacol. Res. 152 (2020) 104609.
[111] R. Roskoski Jr., Guidelines for preparing color figures for everyone including the colorblind, Pharmacol. Res. 119 (2017) 240–241 Erratum in: Pharmacol Res. 2019;139:569.